

Université de Montréal

**Design of minimally invasive diagnostic and dermal fluids sampling
microneedle**

Presented by :
Naghme Rezania

Analyse et Formulation des Médicaments
Faculté de Pharmacie

Mémoire présentée à la Faculté de Pharmacie
en vue de l'obtention du grade de Maîtrise en Sciences Pharmaceutiques
Option Technologie Pharmaceutique

Septembre 2023

© Naghme Rezania, 2023

Université de Montréal

Axe Analyse et Formulation du Médicament, Faculté de Pharmacie

Ce mémoire intitulé

**Design of minimally invasive diagnostic and dermal fluids sampling
microneedle**

Présenté par

Naghme Rezania

A été évalué par un jury composé des personnes suivantes

François-Xavier Lacasse

Président-rapporteur

Davide Brambilla

Directeur de recherche

Xavier Banquy

Codirecteur de recherche

Gregory De Crescenzo

Codirecteur de recherche

Gaétan Mayer

Membre du jury

Résumé et contexte

Ce mémoire de maîtrise porte sur le développement de microaiguilles hydrogels pour la capture et la détection précoce de biomarqueurs protéiques spécifiques du liquide interstitiel cutané. Le diagnostic précoce d'une maladie et le suivi préventif des paramètres biologiques peuvent effectivement améliorer les traitements et auront un rôle plus important dans les années à venir. Cependant, des obstacles considérables à cette approche persistent, en particulier la nature hautement invasive et perturbatrice des analyses biologiques. Se rendre dans une clinique et subir un prélèvement invasif de sang (ou de liquide biologique) sont des défis considérables par rapport aux traitements courants, qui consistent souvent en des médicaments qui peuvent être pris sans douleur à la maison.

Une solution à ces problèmes peut être trouvée dans l'invention de méthodes peu invasives pour le diagnostic et l'analyse des soins de santé, idéalement celles qui peuvent être utilisées à domicile sans nécessiter de personnel formé. À cet égard, les micro-aiguilles (MNs) démontrent un énorme potentiel car leur petite taille garantit qu'elles sont relativement simples et presque indolores. De plus, leur nature simple et à usage unique permet potentiellement une administration à domicile par le patient. Les micro-aiguilles d'hydrogel présentent des caractéristiques bénéfiques à des fins de diagnostic compte tenu de leurs propriétés de gonflement qui permettent d'absorber les fluides corporels tels que le liquide interstitiel (ISF) et de capturer les biomarqueurs. Ces caractéristiques remarquables ont poussé les scientifiques à utiliser des micro-aiguilles d'hydrogel pour des applications de diagnostic.

Afin de fournir un contexte pour le développement de cette technologie, cette thèse commence par un examen des principes et des avancées récentes dans le domaine des applications diagnostiques des MN (**Chapitre 1**). Par la suite, des sections expérimentales, de résultats et de discussion seront présentes sur la fonctionnalisation de l'hydrogel avec des anticorps pour la détection de biomarqueurs spécifiques (**Chapitre 2**). Le dernier chapitre aborde la conclusion générale et les perspectives d'avenir de cette approche (**Chapitre 3**).

Mot-clé : Liquide interstitiel, microaiguilles hydrogel, anticorps, diagnostic.

Summary and Context

This master's thesis focuses on the development of hydrogel microneedles (HMNs) for capture and early detection of specific protein biomarkers from the skin interstitial fluid. Early disease diagnosis and preventative monitoring of biological parameters can effectively improve medical results and anticipate playing a more important part in the forthcoming years. However, considerable barriers to this approach persist, specifically the highly invasive and disruptive nature of biological analyses. Visiting clinics and undergoing invasive blood (or biological fluid) sampling are considerable challenges in comparison with common treatments, which often consist of drugs that may be taken painlessly at home.

A solution to these concerns can be found in the invention of minimally invasive methods for diagnostics and healthcare analyzing, ideally ones that may be utilized at home without the requirement for trained staff. In this regard, microneedles (MNs) demonstrate tremendous potential as their small size ensures that they are relatively straightforward and almost painless. Also, their simple and single-use nature potentially permits at-home administration by the patient. HMNs demonstrate beneficial features for the diagnosis purposes considering the swelling properties of them which give the chance of absorbing body fluids such as ISF and capture of the biomarkers. These remarkable features have driven scientists to employ HMNs for diagnostic applications.

To provide background for the development of this technology, this thesis begins with a review of the principles and recent advances in the field of diagnostic applications of MNs (**Chapter 1**). Subsequently, experimental, result, and discussion sections will be present about the functionalization of hydrogel with a model antibody for specific biomarkers detection (**Chapter 2**). The last chapter discusses the general conclusion and future prospects of this approach (**Chapter 3**).

Keyword: Interstitial fluid, hydrogel microneedles, antibody, diagnosis.

Abstract

Precise diagnosis enables early detection of diseases and improves patient outcomes by guiding effective medical interventions. The advancement of precision medicine in the future will undoubtedly rely on the identification of validated biomarkers. A better understanding of these biomarkers is required to accurately categorize patients based on their expected disease risk, prognosis, and response to particular treatments. Recent advancements in medical diagnostics include the use of hydrogel microneedles, which provide a minimally invasive and patient-friendly method for collecting interstitial fluid for biomarker analysis. Their unique swelling capability upon contact with bodily fluids enables efficient fluid extraction while maintaining patient comfort. Furthermore, the porous structure of them eases the incorporation of biomolecules such as antibodies and aptamers, serving the purpose of detection upon insertion into the skin. This innovative approach holds promise for real-time and non-invasive diagnostics, allowing for early disease detection and personalized healthcare.

Table of Contents

Content

Chapter 1	15
1. Introduction	16
1.1. Skin structure.....	17
1.2. Interstitial Fluid (ISF).....	18
1.3. Techniques of ISF extraction.....	19
1.3.1. Suction blister technique.....	19
1.3.2. Sonophoresis	20
1.3.3. Reverse ionophoresis	20
1.3.4. Thermal ablation	20
1.3.5. Microdialysis and ultrafiltration	21
1.3.6. Needle-based extraction.....	21
1.4. Biomarkers	22
1.5. Techniques for Biomarker Detection	22
1.5.1. Gel electrophoresis.....	22
1.5.2. Immunoassay-based technique	23
1.5.3. Enzyme-linked immunosorbent assay (ELISA)	23
1.5.4. Electrochemical immunoassay.....	23
1.5.5. Surface enhanced Raman spectroscopy (SERS).....	24
1.5.6. Fluorescence-based detection	24
1.6. Microneedles	24
1.7. Different types of MNs	25
1.7.1. Solid microneedle	25

1.7.2.	Coated MNs	26
1.7.3.	Hollow MNs.....	26
1.7.4.	Dissoluble MNs	27
1.7.5.	Hydrogel MNs	27
1.8.	MN fabrication techniques	28
1.8.1.	Laser Mediated Fabrication Techniques	29
1.8.1.1.	Laser Cutting.....	29
1.8.1.2.	Laser Ablation.....	29
1.8.2.	Photolithography.....	29
1.8.3.	Additive manufacturing (3D printing)	29
1.8.3.1.	Microstereolithography (μ SL)	30
1.8.3.2.	Continuous liquid interface (CLIP)	30
1.8.3.3.	Two-photon polymerization (TPP)	30
1.8.4.	Fabrication of polymeric MNs using solvent.....	30
1.8.4.1.	Micromolding	30
1.8.4.2.	Automized spraying to fill molds.....	31
1.8.5.	Droplet-born air blowing (DAB)	31
1.9.	Application of MNs.....	31
1.9.1.	Drug delivery.....	31
1.9.1.1.	Protein Delivery	32
1.9.1.2.	Vaccine delivery	32
1.9.2.	ISF extraction	33
1.9.3.	Diagnosis	34
1.9.3.1.	Biomolecule functionalization of MNs.....	35
1.10.	References	37

Hypothesis and Research Objectives	42
Chapter 2.....	43
2.1. Abstract.....	45
2.2. Introduction	46
2.3. Materials and methods	47
2.3.1. Materials	47
2.3.2. Characterization.....	48
2.3.4. Labeling of BSA and IgG with Cy5 fluorescence dye	49
2.3.5. Functionalization of HSSs with protein molecules (BSA and IgG)	50
2.3.5.1. Application of Copper free Click Chemistry	50
2.3.5.2. Application of EDC/NHS	51
2.3.6. Validation of the functionalization using fluorescent labeled sABs.....	53
2.3.7. Modifying hydrogel formulation.....	53
2.3.7.1. Functionalization of modified hydrogel formulation (MHF) with IgG-Cy5 using EDC/NHS at high concentration.....	54
2.3.8. Validation of functionalization using sABs	54
2.3.9. Mechanical properties of hydrogel	55
2.3.10. Swelling ratio of hydrogel MNs	55
2.3.11. Capture protein biomarker using HMNs	56
2.4. Results and discussion.....	56
2.4.1. Synthesis of hydrogel free-needle samples and HMNs.....	56
2.4.2. Labeling of BSA and IgG with Cy5 fluorescence dye	59
2.4.3. Functionalization of hydrogel using copper-free click chemistry	60
2.4.4. Functionalization of hydrogel with IgG using EDC/NHS chemistry.....	63
2.4.5. Validating the functionalization using labeled secondary antibody	66

2.4.6. Characterization of MHF samples	67
2.4.7. Functionalization of MHF samples	68
2.4.7.1. Validation of functionalization with secondary antibody	69
2.4.8. Mechanical properties of hydrogel	69
2.4.9. Swelling properties of hydrogel	70
2.4.10. Capture BSA with the functionalized hydrogel	71
2.5. Conclusion.....	72
2.6. References	73
Chapter 2 -Supporting Information.....	76
Chapter 3	78
3.1. Conclusion and outlook.....	78
3.2. References	81

List of figures

Chapter 1

Figure 1-1. Schematic of skin layers.....	18
Figure 1-2. Indirect sandwich model ELISA.....	23
Figure 1-3. Schematic of the insertion of HMNs into the skin.....	28
Figure 1-4. Disease detection and monitoring using microneedle.....	35

Chapter 2

Figure 2-1. Hydrogel formulation and samples shape.	58
Figure 2-2. Cy5 excitation and emission.	60
Figure 2-3. Functionalization of hydrogel using copper free click chemistry.	62
Figure 2-4. Functionalization of hydrogel using EDC/NHS.	64
Figure 2-5. Morphology and functionalization of MHF samples.	68
Figure 2-6. Characterization of MHF samples.	71
Figure 2-7. Capture and detection of BSA.....	71
Figure 2-S1. Two various conditions for hydrogel functionalization with BSAs.....	76
Figure 2-S2. TLC result	76
Figure 2-S3. Hydrogel morphology after functionalization.	77
Figure 2-S4. MNs after mechanical test	77

List of Tables

Chapter 2

Table 1. FTIR peaks correspond to synthesized hydrogel.....57

List of Abbreviation

BNP- Brain natriuretic peptide

BSA- Bovine serum albumin

CAD- Computer Aided design

CLIP- Continuous liquid interface

COOH- Carboxylic acid

CS- Chitosan

Cy5- Cyanine 5

DAB- Droplet-born Air Blowing

DBCO- Dibenzo cyclooctyne

DMSO- Dimethyl sulfoxide

DNA- Deoxyribonucleic acid

EDC- 1-Ethyl-3-(3-dimethylaminopropyl) carbodiimide

ELISA- Enzyme linked immunosorbent assay

FITC – Fluorescein isothiocyanate

HMNs- Hydrogel MNs

HSSs- Hydrogel square samples

ISF- Interstitial fluid

IgG- Immunoglobulin G

MHF- Modified hydrogel formulation

MNs- Microneedles

NHS- N- hydroxy Succinimide

NH₂- amine

NT-proBNP- N-terminal propeptide B-type natriuretic peptide

PEG-Polyethylene glycol

PAA-Polyacrylic acid

pABs- Primary antibodies

PHVE/ME- Poly (methyl vinyl ether-co-maleic anhydride)

PEG- Polyethylene glycol

POC- Point of Care

PVA- Polyvinyl Alcohol

RNA- Ribonucleic acid

sABs- Secondary antibodies

SEM- Scanning electron microscopy

SERS- Surface enhanced Raman spectroscopy

3D- Three dimensional

TLC- Thin Layer Chromatography

TPP-Two-photon polymerization

UV- Ultraviolet

Acknowledgement

During the period of study at Université de Montréal, I have gained many experiences working with many people. Hereby, I wish to express my heartfelt thanks to them all in my humble acknowledgement. I am deeply grateful to my advisor, **Prof. Davide Brambilla**, for their unwavering guidance, valuable insights, and continuous support throughout conducting this research., He has been very patient and offered invaluable guidance and assistance. My genuine appreciation also goes to **Prof. Xavier Banquy** who provided me constructive suggestion and access to his lab facilities. Also, I would like to thank **Prof. Gregory De Crescenzo** for his support. I extend my thanks to the members of my thesis committee for their valuable feedback, constructive criticism, and insightful suggestions that significantly enhanced the quality of this work. I also like to thank all my friends and lab mates especially Sina Salimi, Hu Zhang, and Samuel Babity who helped me during my journey. I sincerely thank my lovely family for their love and support during these years, although they were far from me, they always tried to their lovely support and help in challenging situation. Lastly, the PrEEmiuM scholarship, as well as access to facilities of the Faculty of Pharmacy at Université de Montréal, are also gratefully acknowledged.

Chapter 1

This chapter will explore the importance of employing interstitial fluid (ISF) as a potentially valuable diagnostic fluid. Next, we will examine different approaches utilized for the extraction of ISF and the subsequent detection of biomarkers. Within this set of methodologies, particular emphasis will be placed on elucidating the current significance of microneedles due to their ability to offer a non-intrusive pathway for accessing ISF and facilitating diagnostic applications.

1. Introduction

The role of a biomedical engineer involves utilizing their scientific expertise to develop technological solutions for health-related issues. In recent years, biomedical engineering research has concentrated on creating innovative tools for medical diagnosis, treatment, and patient monitoring, all aimed at improving the management of various health conditions. The significance of early disease diagnosis cannot be underestimated as it plays an important role in choosing the right medical treatments and preventing long-term health problems; indeed, achieving a precise diagnosis is the initial crucial step towards receiving effective treatment [1]. For instance, delayed diagnosis of infectious diseases like HIV and tuberculosis heightens the risk of transmission and complicates their treatment.

Body fluids play a pivotal role in the field of diagnosis due to the wealth of information they hold about the body's health and function. These fluids, including blood, urine, saliva, and interstitial fluid (ISF), can contain various molecules, cells, and biomarkers that provide insights into the presence, progression, and severity of diseases. Detecting changes in these biomarkers can help diagnose diseases even before noticeable symptoms appear.

Blood is a valuable body fluid that contains a wealth of information about a person's health, including the levels of different molecules, cells, and biomarkers. Blood sampling is a traditional diagnostic approach for the wide range of medical conditions. However, its invasive nature often leads to patient discomfort, skin injury, and damage. Moreover, some individuals experience irritation and intolerance towards the process. Consequently, there is a growing demand for non-invasive techniques to address these challenges and enhance patient comfort during diagnostics [1, 2].

In recent years, there has been significant interest in the biomedical community regarding the collection and detection of biomarkers from skin ISF. This is primarily due to the non-invasive nature of accessing ISF compared to blood samples. The ISF consists of a diverse range of indicators, including small molecules and proteins, and it is typically found in the dermis layer of the skin.

Among the various methods of ISF extraction, microneedle (MNs) technology has emerged as a prominent approach. This technique involves the creation of micro-holes in the skin to facilitate

the collection of ISF; particularly, hydrogel microneedles (HMNs) demonstrate exceptional characteristics [1].

Moreover, developing diagnostic tools that patients can use at home has become increasingly important for several compelling reasons. Home diagnostic tools allow individuals to regularly monitor their health status, enabling early detection of potential issues. This proactive approach can lead to timely intervention and better disease management. Furthermore, it eliminates the need for patients to travel to a healthcare facility, and reducing the inconvenience associated with appointments and waiting times. Many chronic diseases also require consistent monitoring of parameters such as blood glucose levels, blood pressure, or cholesterol. Therefore, home diagnostic tools empower patients to manage their conditions effectively. There exist numerous more benefits associated with these tools that have the potential to enhance the quality of individuals' lives in the future. The emergence of MNs in the field of medical diagnosis marks a significant advancement that has revolutionized traditional diagnostic approaches. MNs, composed of tiny, needle-like structures, have introduced a new era of minimally invasive and patient-friendly diagnostics. These innovative tools penetrate the outermost layer of the skin, reaching the ISF beneath, which holds a wealth of diagnostic information. Unlike conventional methods that often require invasive procedures, MNs enable painless and efficient sampling of ISF, making them ideal for various diagnostic applications.

HMNs possess a remarkable dual capacity, serving not only for the extraction of ISF but also for detection purposes. Their porous structure enables them to enlarge in the presence of body fluids and provides additional space for biomolecule functionalization. The future holds great promise for HMNs as a minimally invasive diagnostic tool which could potentially replace hypodermic needles, offering a solution to the pain, injury, and discomfort often linked with their use.

1.1. Skin structure

Anatomically, the skin is the largest and heaviest organ in the human body and contain 15% of their weight, with a thickness of typically 2 mm. However, this may vary based on anatomical location, a person's age, and sex. The skin is responsible in protecting the body from external physical, chemical, and biological attacks, preventing excessive water loss, and maintaining body

temperature [3]. Skin is made up of three main layers: epidermis, dermis, and hypodermis. A group of cells called keratinocytes make up the epidermis, the top layer of the skin. Keratin is a protein with a thread-like structure that serves as a protective material. Dermis, the middle layer, is mostly composed of collagen fibrils; it is located between the epidermis and subcutaneous tissue and is made up of small lobes of fat cells called lipocytes. Skin's thickness is different based on where the body is located and how it was constructed. Approximately, 0.1 mm of epidermis covers the eyelids, making them the thinnest skin on the body. Comparatively, the palms of the hands and soles of the feet have the thickest skin, measuring about 1.5 mm thick. On the back, the dermis is 30 to 40 times thicker than the epidermis. In recent years, the collection and detection of biomarkers from ISF of the dermis layer of the skin have gained considerable attention in the biomedical fields due to its non-invasive access compared to blood samples. Based on these findings, ISF comprises a variety of indicators, ranging from tiny molecules to proteins. The composition of these biomarkers is intimately related to the physiological function of organisms and may represent the health situation [3-8].

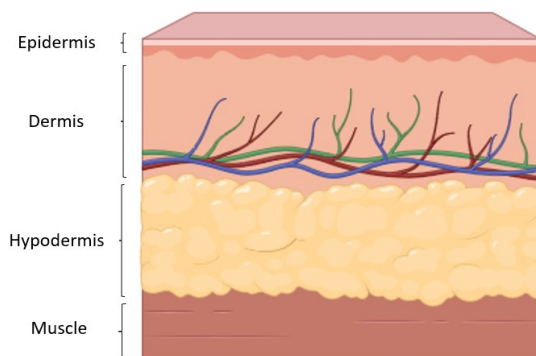


Figure 1-1. Schematic of skin layers; it includes three main layers: epidermis, dermis, and hypodermis.

1.2. Interstitial Fluid (ISF)

The increasing interest in personalized medicine and point-of-care (POC) diagnostics centers around biomarkers. Blood, the primary source of these biomarkers, is often collected through painful venipuncture, requiring skilled medical professionals. While urine and saliva are more accessible, they have limitations - urine biomarker levels fluctuate due to circadian rhythms, and saliva-based assays may be affected by food or drugs [9, 10].

ISF is a body fluid which is located primarily in the skin's dermis layer and surrounds cells in tissue gaps. The ISF appears to be the most ideal human body fluid for the minimally invasive detection of biomarker; it is unquestionably a more accessible and repeatable matrix [6, 7, 11, 12]. The information included in these biomarkers is intimately related to organisms' physiological function and may provide insight into health situation [4]. Capture and detection of biomarkers from ISF have attracted increasing interest in the biomedical fields because of the non-invasive and simple sampling method, as well as the existing pathways of multiple blood biomarkers into the highly vascularized dermal layer [12].

To avoid repeated blood sampling from patients, dermal ISF is preferable as a measuring medium for physiological information. It is possible to reach dermal or subcutaneous ISF through the skin, however extraction techniques are not practical for therapeutic usage. Blood may be collected directly from a patient in less than three minutes, but ISF extraction reports indicate varying waiting times ranging from ten minutes to several hours [12]. Depending on the instrument and extraction procedure, ISF extraction also gives small sample volumes. Conventional methods of accessing ISF through the skin have not been fully developed and pose a technological challenge.

1.3. Techniques of ISF extraction

As discussed before, ISF is an alternative to blood that contains biomarkers for the early detection of disease; it also offers non-invasive pathway for early diagnosis. There are some ISF extraction techniques including suction blister, wick implantation, tissue cage reservoir, skin window technique, sonophoresis, reverse ionophoresis, thermal ablation, microdialysis and MNs.

1.3.1. Suction blister technique

Typically, the extraction of dermal ISF requires an external force, such as mechanical pressure or vacuum generated by negative pressure. This is the primary method of ISF extraction which was developed by Kiistala et al. This technique creates a gap between the epidermis and dermis and draw ISF to the skin's surface [12-14]. If this treatment by this technique is continued for around 2 hours, a separation of the dermis and epidermis may take place and lead to the formation of blister; the collected fluid inside it is called suction blister fluid (SBF) which is a trustable source for the analysis of ISF.

There are some challenges that come with this technique which includes the inflammation around the blister, various blister sizes and collected ISF. In addition to these challenges, this technique is also time consuming as the ISF diffusion through dermis and epidermis is quite slow. Also, applying higher negative pressure causes damage to the extraction area and also bleeding which enter contamination into the sample [12, 15]

1.3.2. Sonophoresis

Sonophoresis generates epidermal micro-vibration by application of vacuum pressure and low-frequency ultrasound. Low-frequency ultrasound makes the skin more permeable since it breaks down the protective function of the stratum corneum. Despite the beneficial features of applying ultrasound and vacuum pump cooperatively in extraction process, the ISF spread over the skin's surface which complicates ISF collection. There is a possibility that the patient's skin will get somewhat heated throughout the procedure. Therefore, the drawbacks of this method restrict its usefulness, and the desire for more research is understandable [14, 16, 17]

1.3.3. Reverse ionophoresis

Ionophoresis is a technique that utilizes a low-level electrical current to enhance the flow of ISF through the skin. Indeed, it employs negatively charged electrode to generate an electric field which leads to the transmission of electrically charged molecules. In a normal situation, the subdermal ions migrate randomly and with nearly constant concentrations. This technique has attracted more attention in terms of glucose monitoring. It also has potential use in the identification and tracking of a wide range of biomarkers. There are, however, certain restrictions on this method. For instance, the running current needs to be adjusted, as excessively high currents might cause skin harm [14, 18].

1.3.4. Thermal ablation

This approach can also be employed for the generation of micropores. In this scenario, the application of a high-frequency electrode on the skin serves to induce the movement of ions within the cells, thereby monitoring changes in the direction of the applied current's orientation. This results in tissue heating and ablation of the stratum corneum in the application region. By

comparison, more ISF ($\approx 0.5 \mu\text{L min}^{-1}$) can be collected by this method whereas the quantity of micropores correlates to the ISF amount. Nevertheless, thermal ablation can cause inflammation, infection, and tissue damage [14].

1.3.5. Microdialysis and ultrafiltration

Microdialysis has been demonstrated to be the most efficient method for obtaining ISF analytes that precisely reflect their concentrations in the dermal tissue layer. Regardless of advances in research, there are no popular clinical extraction techniques to analyze transdermal fluid. Microdialysis and ultrafiltration are among the beneficial techniques for ISF sampling with the intention of diagnosis. The principle behind these two methods is the usage of semipermeable membrane at the target area. In microdialysis, the drug molecules move across the membrane while in the ultrafiltration by employing vacuum it is possible to extract drug molecules. Long-term implantation of ultrafiltration probes has been indicated to yield collection rates of up to $50 \mu\text{l h}^{-1}$; Nonetheless, they depend on the extremely painful insertion of a large trocar into the epidermis. In both approaches, membrane contamination is a matter of concern [12, 14, 18].

1.3.6. Needle-based extraction

A less complex approach for collecting ISF entails the insertion of a needle with a small diameter into the dermal layer, followed by the application of pressure nearby the needle. Typically, a circular apparatus is utilized to reduce skin compression surrounding the MNs, resulting in decreased fluidic hindrance and enhanced extraction. The technique facilitates the collection of fluid volumes of up to approximately $1 \mu\text{l}$ within a matter of seconds [18]. A novel version of the needle-based technique involves the utilization of MNs patches coated with receptors to capture target analytes in situ. This is followed by the removal of the patch and ex vivo analysis, preventing the need of collecting large fluid volumes. Currently, MNs have received a greater spotlight in the field of health and medicine simply because they offer a non-invasive way to acquire ISF, which is more effective for the patient. In the subsequent sections, more detail will be presented to support the advantage of MNs compared to conventional methods for the body fluid sampling and the field of diagnosis.

1.4. Biomarkers

Biomarkers play a vital role in disease detection and treatment follow-up. The complete potential of biomarkers remains largely untapped due to existing technological challenges in effectively detecting them. Biomarkers are often present at very low concentrations mixed with other proteins, making it more difficult to identify them. Hence, it is often challenging and time-consuming to detect biomarkers at very low concentrations. Early detection of biomarkers leads to more success in the treatment of the disease specially in the case of cancer, cardiovascular disorder and other pathological condition [19]. For instance, many people around world suffer from heart failure and cardiac dysfunction and the number of them is promptly increasing by their age. Therefore, the concentration of some related biomarkers such as brain natriuretic peptide (BNP) and N-terminal propeptide B-type natriuretic peptide (NT-proBNP) increase in the body. Early detection of these biomarkers gives the chance of early treatment and prevent the progression of cardiac disease [20, 21].

1.5. Techniques for Biomarker Detection

The principal aim behind the biomarker detection is developing reliable and cost-effective tools for early diagnostic of disease that assist physician to choose more precise and accurate therapy. Moreover, it might help them within successfully tracking disease progression and recurrence. In this regard, there are various methods of biomarker's detection which most of them are immunoassay based methods [19].

1.5.1. Gel electrophoresis

A typical method for protein separation is gel electrophoresis using the molecular weight of the protein. It is a rapid, simple, and highly sensitive tools. Generally, the sample is run into the support matrix such as agarose or polyacrylamide gel. The separation happens by migration of charged molecules through the matrix upon application of electric fields usually provided by the immersed electrodes [22-24].

1.5.2. Immunoassay-based technique

Immunoassay relies on the interaction between primary antibodies (pABs) and specific antigens. This binding is subsequently complemented by the attachment of secondary antibodies (sABs) to unoccupied antigen sites. The precision and sensitivity of immunoassays are contingent upon the effectiveness of the binding between pABs, sABs, and biomarkers such as antigens. One of the popular immunoassay techniques is enzyme-linked immunosorbent assay (ELISA) [25].

1.5.3. Enzyme-linked immunosorbent assay (ELISA)

ELISA commonly utilizes animal-derived antibodies that are targeted towards certain biomolecules. This technique is highly valuable for identifying and quantifying biomarker proteins in biological fluids and serum. Sandwich ELISA is formed when the enzyme-linked sABs bind to the other epitope of antigen and leading to the conversion of the substrate into a colored product. The intensity of the color is directly correlated to the amount of enzyme linked antibody and, therefore, to the amount of antigen bound to the immobilized pABs. The issue with ELISA-based methods is the precision, as the reliability of this test heavily depends on how the primary antibodies (pABs) are attached to the surface through immobilization chemistry [19]. Figure 1-2 illustrates the capture of antigen with pABs and detection of it by adding enzyme-linked sABs to the other part of the antigen's epitope which leads to formation of direct sandwich ELISA.

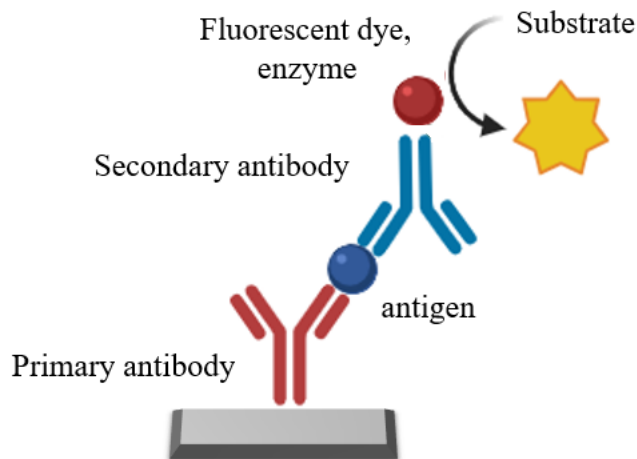


Figure 1-2. Direct sandwich model ELISA: Detection of biomarker using ELISA which includes primary antibody (pAB) and secondary antibody (sAB).

1.5.4. Electrochemical immunoassay

Electrochemical sensors have exhibited significant promise in the identification of biological indicators like viruses and disease-related pathogens such as hepatitis B and HIV. While point of care (POC) sensors have certain limitations, such as insufficient sensitivity and lack of data quantification, the integration of electrochemical detection offers the potential to enhance sensitivity and enable the acquisition of quantitative measurements. The most prevalent example of electrochemical sensors are portable glucometers, which are routinely used by diabetic patients to measure their blood glucose levels [27,26]

1.5.5. Surface enhanced Raman spectroscopy (SERS)

SERS is a spectroscopic technique that exhibits high sensitivity in detecting biomarkers. It has the potential to be employed for the purpose of protein biomarker identification approximately close or on the surface of a plasmonic nanostructure. The success of this method crucially depends on scattering cross-section of immobilized molecule on the metallic nanostructures. Consequently, the efficacy of SERS is influenced by metallic nanostructures and the immobilization of antibodies on stated structures [19, 28, 29].

1.5.6. Fluorescence-based detection

Fluorescence detection has emerged as a prominent optical method extensively employed in biological applications. This approach enables the straightforward quantification of biomarker proteins, facilitates the detection of large-scale samples, and offers convenient labeling of biomolecules using fluorescent tags. In the quantification of antigens within samples, fluorescently labeled sABs are utilized. Fluorescence-based techniques encompass various detailed methods, including flow cytometry, quantum dot technology, protein microarray, etc. [19].

1.6. Microneedles

The employment of MNs platforms for interfacing with ISF has gained significant attention as a promising approach for extracting tissue fluid from the dermis. MNs are a safe, efficient, and effective tool with the tiny needles (150–1500 μm in height, a width of 50–250 μm , and a tip thickness of 1–25 μm , and up to 2000 MN cm^2) usually organized in an array to pass stratum

corneum layer of the skin without feeling any pain or bleeding. It offers a minimally invasive route for the transdermal delivery of medicines that are typically too large to be absorbed through skin [4, 12, 30]. Another critical application of MNs is body fluid sampling [31]. MNs were first introduced by Prausnitz and coworkers with the intention of drug and vaccine permeation across the stratum corneum. The headmost MN product that was commercially accessible in 2006 was created by Dr. Desmond Fernandes which is now known as the Dermalroller; its objective was to introduce solid microneedles to create small pathways in the skin, improving skincare absorption [30].

Although most of the studies has focused on the application of MNs for drug and vaccine delivery throughout the skin, some current studies take more attention to their application for the detection of chemical analyte in the body such as glucose, glutamate, and lactic acid [32] which give doctors important diagnostic information.

When compared to alternative continuous monitoring systems, MNs offer several advantages. Firstly, their small size makes them minimally invasive upon insertion. Additionally, these arrays are replaced daily, typically within 24 to 48 hours, which is shorter compared to other devices that require implantation for a longer period, usually 7 to 14 days [11]. Furthermore, due to their less invasive nature, MNs minimize skin irritation, discomfort, and tissue stress. They also reduce the risk of local infection, bleeding, and promote faster skin recovery within 24 hours or less [33].

1.7. Different types of MNs

There are various types of MNs including solid, coated, hollow, dissoluble and HMNs which can be made of various materials such as glass, metal, coated metal, silicon, solid polymer, aqueous hydrogel, and dissolving polymer [30, 34].

1.7.1. Solid microneedle

Solid MNs penetrates the stratum corneum to increase the drug's bioavailability and kinetic transport across the skin. Compared to intramuscular delivery, solid MNs are suitable for vaccine administration because they persist longer and elicit a stronger antibody response. Solid MNs are simpler to produce, have greater mechanical qualities, and have sharper tips than hollow MNs. In

addition, the solid MNs can be manufactured from a variety of substances, including silicon, metals, and polymers [35-39].

1.7.2. Coated MNs

Coated MNs are solid-type MNs covered with medications. Depending on the thickness of the coating layer, it often contains a lower concentration of the active ingredient. The capacity to reliably coat MNs with a regulated drug layer is crucial to the efficacy of medication delivery. A coated MNs has the capability to deliver proteins and DNA in a minimally invasive manner. While the rapid administration of medication to the skin stands as an advantage of these coated MNs, it's important to note that the presence of drug residues at the needle's tip could potentially lead to cross-contamination among different patients. In conclusion, the outcomes of vaccine administration through the use of coated MNs were found to be comparable to those achieved through intradermal and intramuscular methods [35, 37-39].

1.7.3. Hollow MNs

Hollow MNs feature a chamber or core that is utilized for injecting or storing medication. Furthermore, these hollow MNs have the capability to transport substantial molecules into the viable epidermis and dermis layers. Unlike solid MNs, these specialized MNs have the capacity to hold larger quantities of medication solutions due to their internal structure [35]. Furthermore, it exhibits the ability to regulate drug release gradually, rendering it a suitable option for liquid vaccines. A hollow MNs operates as an active drug delivery system, releasing drugs from a reservoir without the need for pressure, in contrast to solid MNs which release drugs through osmotic gradients. The release kinetics of hollow MNs can be adjusted by manipulating both material composition and fabrication parameters. However, these hollow MNs have garnered less attention compared to solid MNs due to their relatively weaker structure and the additional attention required in terms of design and insertion procedures. Additionally, technical challenges such as leaks and clogs during the injection process are associated with the use of hollow MNs [35, 37-39].

1.7.4. Dissoluble MNs

According to their characteristics, dissolvable MNs are considered as a promising technique that has been available since 2005. The advantage of this kind of MNs is facilitating the rapid release of macromolecules as well as the ease of application of drugs through one-step procedures. By dissolving the needle tip after insertion into the skin, the loaded drug releases and diffuses easily. The design and production of a dissolvable MNs require technical expertise. However, in terms of suitable material and technique for dissolving MNs fabrication, water-soluble material and micro-mold fabrication were considered as the most suitable one for both of them [35, 37-39].

1.7.5. Hydrogel MNs

The most recent kind of MNs, known as HMNs, was initially identified in 2012 [40]. HMNs provide unique advantages compared to other technologies. Their versatile design, self-disabling capability, and minimal risk of blockage offer clear benefits over alternative MN approaches used for monitoring purposes. Apart from their biocompatibility and biodegradability, these MNs can remain intact and are removed without leaving any residue, even though they soften due to the absorption of ISF. Significantly, when compared to dissolving and coated MNs that may leave residual substances on the patient's skin, which could potentially lead to irritation or sensitization, HMNs do not leave any detectable polymer residue on the patient's skin. Moreover, HMNs do not face the challenge of skin tissue compression that often arises with hollow MNs. Unlike solid and hollow MNs, HMNs offer a one-step application approach for medication administration or ISF removal, which proves to be more efficient and convenient [30, 32]. Comprising crosslinked hydrogel, HMNs exhibit a distinct mode of operation compared to previously mentioned types of MNs [41]. The HMNs possess a hydrophilic nature that grants them the impressive capacity to effortlessly swell upon being inserted into the skin, allowing them to absorb water. This remarkable attribute makes them highly suitable for a wide range of biomedical uses, including aiding in the uptake of ISF. Another benefit of HMNs over traditional MNs is their ease of fabrication in various geometries. They can undergo disinfection prior to insertion and can be retrieved from the skin with greater ease, causing less damage to both the MNs and the skin. Due to their microscale size, HMNs are classified as minimally invasive, as they don't penetrate deeply enough into the skin to activate pain receptors located in the deeper dermal layer. These characteristics could potentially

overcome the limitation of traditional MNs [30, 32]. Taking these factors into account, the current trend in MNs advancement has resulted in the creation of HMNs [12, 30, 37-39]. HMNs possess a wide range of functions, encompassing the extraction and analysis of ISF, the delivery of drugs via the skin, the treatment of skin cancer, the administration of antibodies, and the facilitation of wound healing [30]. Numerous reviews and articles have focused on the utilization of HMNs for extracting ISF and detecting biomarkers [9, 30, 32, 40, 42-44]. Consequently, the potential of HMNs as a minimally invasive method is inspiring for the future, as it could eliminate the use of hypodermic needles, prevent pain, injury, and irritation associated with their application [32].

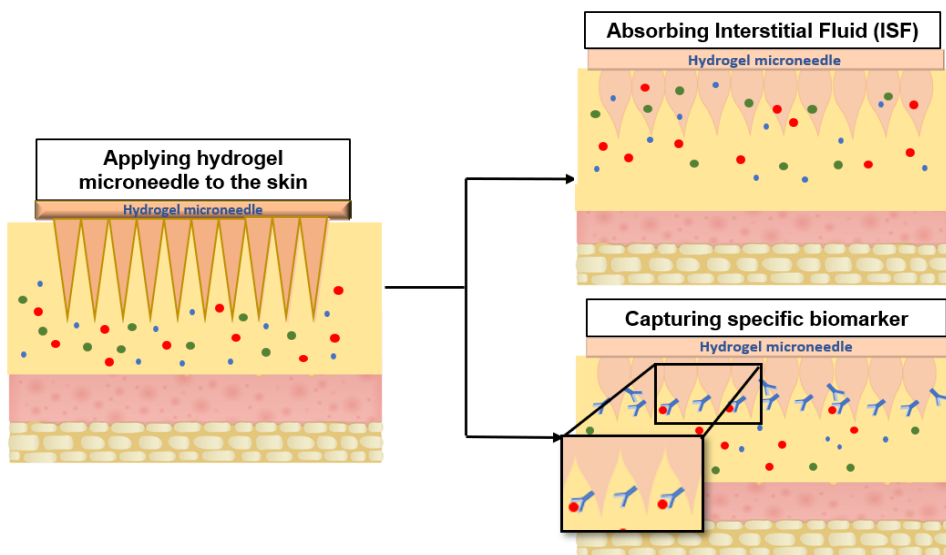


Figure 1-3. Schematic of the insertion of HMNs into the skin; it can be used for two various applications including extraction of ISF and detection of biomarkers in ISF.

1.8. MN fabrication techniques

This section delves into the diverse MN fabrication techniques, exploring the cutting-edge methods and technologies used to create these micron-sized structures. Various approaches are explored in detail. The advancement of these fabrication techniques has revolutionized the field, allowing for the precise control of MNs size, shape, and material composition, thus paving the way for enhanced drug delivery efficiency and therapeutic efficacy.

1.8.1. Laser Mediated Fabrication Techniques

1.8.1.1. Laser Cutting

This method employs an infra-red laser to cut the sheet, precisely removing the metal based on a computer-aided design (CAD), which produces flat MNs on the sheet. Following this, the fabricated MNs are cleaned and bent at a 90° angle from the sheet. Finally, the tips undergo further refinement using electropolishing [38, 45].

1.8.1.2. Laser Ablation

This technique is applicable not only for the fabrication of metallic MNs but also for polymeric ones. It involves using a laser beam to apply precise engraving onto a plate, shaping it into a three-dimensional structure to create the MNs [38, 45].

1.8.2. Photolithography

Photolithography, a well-known fabrication technique, is used to elaborately create solid or hollow MNs. This technique is utilized in the manufacturing of silicon, dissolving, and HMNs through the creation of an inverse mold that replicates the MN's structure. This approach allows for the fabrication of solid MNs with diverse shapes and customized lengths [38, 46]. In 2021, Dardano et al. documented the single-step creation of HMNs based on polyethylene glycol diacrylate (PEGDA) employing the technique of direct photolithography [46].

1.8.3. Additive manufacturing (3D printing)

Additive manufacturing technology such as 3D-printing lead to highly efficient and cost-effective rapid prototyping of samples. The present technique facilitates the conversion of a three-dimensional computer-aided design (CAD) model into a physical object hence facilitating the construction of various structures, prototypes, and architectural designs through layer-by-layer process [38, 45, 47]. During the past few years, the application of 3D printing technology has extended to the production of microstructures, including MNs. The forthcoming section will delve into diverse classifications of 3D printing methodologies employed for the construction of MNs.

1.8.3.1. Microstereolithography (μ SL)

Micro-stereolithography (μ SL) serves as a high-throughput fabrication methodology with applications in biomedical and tissue engineering. This technique produces three-dimensional microstructures by progressively adding material from the base, achieved through precisely regulated solidification of a liquid medium through photopolymerization processes. The process involves laser beam patterning on a resin surface, followed by layer separation, realignment, and curing to construct a solid, three-dimensional object [38, 45].

1.8.3.2. Continuous liquid interface (CLIP)

It is an additive manufacturing process that allows for the continuous creation of objects using a liquid photopolymer resin. CLIP is distinct from traditional layer-by-layer 3D printing methods, as it utilizes a liquid interface to build the object continuously, allowing for faster production and smoother surface finishes. The process employs a combination of light and oxygen to control the curing of the resin, which results in the precise and rapid formation of complex geometries [38, 45].

1.8.3.3. Two-photon polymerization (TPP)

Two-photon polymerization (TPP) is a sophisticated 3D-printing technique that enables high-resolution fabrication of complex microstructures and nanoscale features. Unlike traditional 3D-printing methods, TPP utilizes ultrafast laser pulses to induce polymerization in a photosensitive resin. This process occurs only at the focal point where two photons simultaneously absorb energy, allowing for the precise and controlled creation of intricate 3D structures [38, 45].

1.8.4. Fabrication of polymeric MNs using solvent

1.8.4.1. Micromolding

Micromolding has been extensively employed in the manufacturing process of dissolving MNs made from materials that are both biocompatible and biodegradable. The process involves uniformly pouring a liquid polymeric solution onto a mold and then removing any air voids. This elimination of air voids can be achieved through vacuum-assisted or centrifugal methods. Subsequently, the molded polymer is dried in an oven before being removed from the mold, resulting in the desired microstructure polymer product [45, 48].

1.8.4.2. Automized spraying to fill molds

By eliminating the requirement for centrifugation or vacuum steps in the micromolding process, the transition to continuous manufacturing, a scalable method, could be significantly simplified. Automated spraying techniques present a potential answer to the difficulties involved with micromolding technique. As a result, these techniques can be employed to apply polymer solutions into molds efficiently without generation of voids [45, 48].

1.8.5. Droplet-born air blowing (DAB)

Droplet-born air blowing (DAB) refers to a technique or process that involves using air blowing to control or manipulate droplets. In this method, droplets are propelled or directed by a stream of air, which can lead to various outcomes depending on the specific application. In this approach, a polymer droplet is transformed into the shape of a MNs using air blowing, enabling a gentle process that avoids the need for external harsh conditions like heat and UV irradiation. Overall, DAB is a versatile technique with applications across various fields where precise manipulation and control of droplets are required [49].

1.9. Application of MNs

The skin, acting as both a formidable barrier and a useful medium for the delivery of bioactive agents, has found significant application in molecular diagnosis and treatment. Traditionally, MNs have been employed to improve drug penetration and transport for disease treatment. Nevertheless, their applications are currently expanding into diverse fields, including immunobiological administration, disease diagnosis, and cosmetic uses [39, 50]. In this section, MNs application in drug delivery, ISF extraction, and detection of various biomarkers will be discussed.

1.9.1. Drug delivery

The stratum corneum presents a challenging barrier for drug delivery. Its protective nature limits the permeation of drugs through the skin, hindering effective delivery to target sites. MNs offer a promising solution by creating microscale channels in the skin, bypassing the stratum corneum and facilitating drug delivery to underlying tissues. In fact, the original applications of MNs in

biomedicine were focused on drug delivery [38, 39, 51]. Through this approach, MNs have the potential to enhance drug absorption and improve therapeutic outcomes which offer a promising platform for delivering proteins, vaccines, antibodies, and other bioactive agents to cure diverse diseases including diabetes, cancers, viral disease, bacterial disease, etc. [52]. The drug is typically deposited either directly onto the MNs tip or onto the surface of the MNs, securely affixed to the base substrate below [38]. There are many literature reviews which present the application of MNs for drug delivery.

1.9.1.1. Protein Delivery

Protein drugs hold immense potential for a wide range of medical applications, including cancer treatments, vaccinations, and the treatment of genetic diseases. Nevertheless, protein delivery faces certain limitations, such as potential alterations in its stability or protein denaturation [38, 50]. For instance, limited therapeutic efficiency may arise during dosing and storage due to protein denaturation, reduced drug absorption efficiency, and restricted cellular permeability associated with the molecular size of the drugs [38]. Chen et al. (2020) presented a remarkable application of glucose-responsive and temperature-stable boronic acid MNs for the purpose of insulin delivery, with the ultimate goal of revolutionizing diabetes treatment [53]. Li et al. (2017) developed solid MNs and investigated their impact on blood glucose levels in diabetic mice upon insulin delivery. The findings showcased a significant reduction in blood glucose levels to just 29% of the initial level after 5 hours, thereby confirming the enhanced permeability of insulin through the skin using the MNs technology [36].

1.9.1.2. Vaccine delivery

Vaccines are medical preparations typically consisting of weakened or inactivated pathogens or their components. These immunogens are administered to individuals to stimulate the immune system, triggering the production of antibodies and immune memory cells. By doing so, vaccines prepare the body to effectively combat specific infections or diseases in the future. Vaccines play a critical role in preventing and controlling the spread of various infectious diseases, thus contributing to public health and saving countless lives worldwide [54]. MNs vaccines present a benefit in enhancing localized immunity by enabling efficient antigen presentation to dendritic cells within the skin. Unlike injectable vaccines, MNs-based formulations can be stored and

transported more flexibly, preserving long-term antigenic immunogenicity without the need for extensive cold storage requirements [38].

1.9.2. ISF extraction

The growing enthusiasm for personalized medicine and POC diagnostics revolves around novel biomarkers. Various health disorders can be effectively monitored and diagnosed by the process of sampling and quantifying different components present in bodily fluids. For example, the quantification of glucose levels can serve as an indicator for the diagnosis of diabetes, while the measurement of cholesterol concentration can be utilised as an indicator for the diagnosis of heart failure [55]. In this regard, extracting ISF has garnered sustained attention as a promising solution to address the limitations associated with capillary blood sampling, urine, and saliva [9, 10]. Due to hydrostatic and osmotic pressures that regulate the outflow of solutes from blood capillaries, the population of small molecules, electrolytes, and proteins in the ISF surrounding dermal cells strongly correlates with plasma [55]. MNs provide a less painful and more accessible method for extracting ISF compared to traditional blood sampling.

Philip R. Miller et al. utilized a hollow MNs to extract significant volumes of ISF approximately 20 μl and 60 μl – without the need for blister formation to puncture the skin. The experiment revealed that ISF started flowing through the capillary within 30 to 120 seconds after application. Subsequently, a greater amount of ISF was collected within 15 minutes, demonstrating the hollow MNs' effective extraction capability for obtaining ISF samples [56]. Mukerjee et al. demonstrated a 20 \times 20 silicon hollow MNs with the length of 250-300 μm (short enough to extract ISF without touch capillary force). The array could penetrate the skin and extract ISF through capillary action into external reservoir. The glucose can be quantified in an extracted ISF as the MNs did not integrate with any detector [57].

Mengjia Zheng et al. utilized HMNs with an added osmolyte for ISF extraction. Although HMNs were capable of extracting ISF, the process took significant time, around tens of minutes, to collect a meaningful volume. By incorporating the osmolyte into the hydrogel, they addressed this issue by creating osmotic pressure that enhanced ISF extraction. Their research demonstrated that these osmolyte-enhanced HMNs extracted three times more ISF compared to regular HMNs. Additionally, the MNs facilitated in vivo quantification of biomarkers like insulin. Furthermore,

when integrated with electronic glucose sensors, the MNs allowed for direct and rapid analysis of extracted glucose, showing their potential for real-time monitoring and diagnostic applications. This innovation represents a significant advancement in MNs technology for efficient and minimally invasive sampling of ISF with potential clinical implications [43]. In another study, Elise et al. introduced a novel acrylic based HMNs, which enabled rapid extraction of ISF for the first time. After sampling with these swelling MNs, they performed proteomic analysis on the extracted ISF. The study demonstrated the successful permeation of the stratum corneum by the MNs, allowing them to collect approximately 6 μ L of dermal ISF within a 10-minute timeframe during in vivo experiments. Through proteomics analysis, a total of 176 clinically significant biomarkers were detected in the collected samples, confirming the suitability of ISF as a relevant bodily fluid for disease monitoring and diagnostic purposes [9]. In another study, He et al. employed HMNs for the purpose of extracting ISF. The MNs was composed of a blend of polyvinyl alcohol (PVA) and chitosan (CS). It has been observed that in all the samples, ISF quantity has increased over the course of time, especially for the sample with a 50/50 ratio of PVA/CS, which was around 2 mg after 2 min and increased to 7.5 mg after 6 min. Increasing the ISF extraction volume can result in an increase in the CS percentage, which in turn increases the porosity and quantity of ISF collected [44].

1.9.3. Diagnosis

It is essential to emphasize that POC devices for detecting analytes other than glucose are not widely established in the commercial market. Moreover, the investigation of analyte levels in ISF, excluding glucose, has not been extensively explored in the academic literature [11]. The use of minimally invasive techniques for extracting ISF has garnered significant attention in the development of HMNs with the primary aim of clinical monitoring and diagnosis [30]. Most MNs only absorb ISF and lack the ability to directly detect biomarkers. Hence, the use of additional technologies such as biosensors, electrodes, and ELISA becomes necessary to differentiate and detect biomarkers, adding complexity to the overall detection process [4]. Biorecognition components, such as receptors, antibodies, and aptamers, are essential for collecting specific analytes from complex biological samples. Therefore, the immobilization of antibodies or aptamers on the MNs surface allows for real-time monitoring of various biomarkers in ISF [58]. Antibodies serve as biorecognition molecules capable of binding exclusively to their associated

antigens. Their exceptional specificity and affinity make them ideal recognition elements for bioassays and sensors. Thanks to these properties, antibodies enable selective binding of analytes (antigens) present in the nano- to picomolar range, even in the presence of numerous other substances, which may surpass the analyte concentration by 2-3 orders of magnitude [27, 58]. Aptamers, single-stranded DNA (or RNA) biomolecules, exhibit antibody-like properties, enabling them to bind to diverse targets. Their application as probes offers highly specific biomarker detection, leveraging their significant advantages such as superior detection specificity, straightforward synthesis, easy modification, and temperature stability in various applications [25].

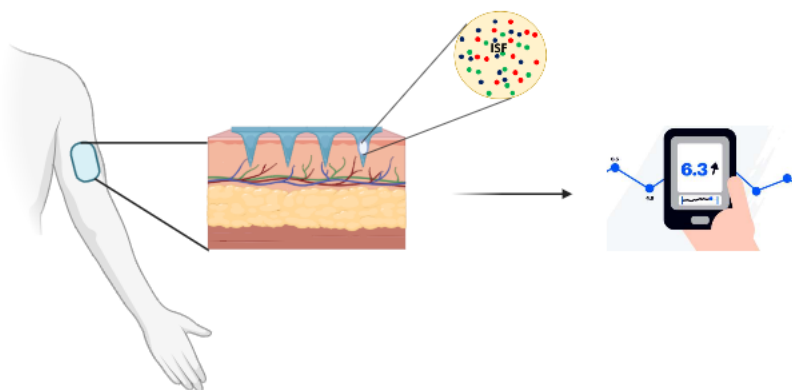


Figure 1-4. Disease detection and monitoring using MNs.

1.9.3.1. Biomolecule functionalization of MNs

Covalently attaching biomolecules to thermoplastic polymers can be achieved through carboxylation. By utilizing carbodiimide chemistry, the carboxylic groups on the surface are activated and can be linked to the amine groups of the biological entities, even after amination. An advantage of this approach over direct amination is the introduction of 1-ethyl-3-(3-(dimethylamino)propyl) carbodiimide (EDC) and N-hydroxysuccinimide (NHS) to the carboxyl groups of the surface before adding biomolecules [59]. Polymers containing carboxylate functions have the potential to easily conjugate proteins using commonly utilized quick conjugation methods, which involve the chemistry of EDC/NHS [60, 61]. EDC-NHS can selectively activate carboxyl groups on the surface of a material, and the resulting NHS esters formed during the reaction are capable of covalently attaching to the amine groups present on target biomolecules. This selective activation and covalent attachment process facilitate the conjugation of

biomolecules to the material's surface [59, 62]. Carboxylation increases hydrophilicity and generates negative charges for electrostatic interactions. The advantages associated with the activation of carboxylic acids and subsequent conjugation to amine groups have contributed to the widespread use of this approach in biomolecular conjugation and protein immobilisation [62]. Xiaoxuan Zhang et al. developed flexible MNs loaded with photonic crystal (PhC) barcodes to detect multiple biomarkers in ISF. The barcodes were immobilized with antibodies using EDC/NHS to enable targeted detection of biomarkers. PhC barcodes of varying colors were employed for the purpose of detection, with each color corresponding to a distinct biomarker. The study provided evidence that the MNs exhibited the ability to selectively capture TNF- α , IL-1 β , and IL-6 biomarkers upon insertion into the abdomen skin of mice. Detection of these biomarkers was achieved by introducing sABs that attach to the opposite side of the antigen. Based on the in-vivo results and a comparative analysis with other detection methods, the researchers have reached the conclusion that the encoded MNs-based detection method holds promise as a potential substitute for blood tests in clinical practise.

In another study, Yi et al (2021). an aptamer decorated MNs was developed for diagnostic applications. The study involved creating porous MNs by integrating glass microspheres into the formulation of the MNs and subsequently etching them out once the solidification process was complete. The researchers successfully developed MNs for diagnostic purposes, enabling the detection of LPS both in vitro and in vivo. They achieved this by immobilizing aptamers within the MNs. The researchers highlighted that the porous structure of the MNs, coupled with the integration of aptamer biomolecules, bestowed them with the capability to effectively detect biomarkers [2].

1.10. References

1. Takeuchi, K. and B.J.N.c. Kim, *Functionalized microneedles for continuous glucose monitoring*. 2018. **5**(1): p. 1-10.
2. Yi, K., et al., *Aptamer-decorated porous microneedles arrays for extraction and detection of skin interstitial fluid biomarkers*. 2021. **190**: p. 113404.
3. Kolarsick, P.A.J., M.A. Kolarsick, and C. Goodwin, *Anatomy and Physiology of the Skin*. Journal of the Dermatology Nurses' Association, 2011. **3**(4): p. 203-213.
4. Zhang, X., et al., *Encoded microneedle arrays for detection of skin interstitial fluid biomarkers*. Advanced Materials, 2019. **31**(37): p. 1902825.
5. Yousef, H., M. Alhajj, and S. Sharma, *Anatomy, skin (integument), epidermis*. 2017.
6. Samant, P.P., et al., *Sampling interstitial fluid from human skin using a microneedle patch*. 2020. **12**(571): p. eaaw0285.
7. Kashaninejad, N., et al., *Microneedle arrays for sampling and sensing skin interstitial fluid*. 2021. **9**(4): p. 83.
8. Hwa, C., E.A. Bauer, and D.E.J.D.t. Cohen, *Skin biology*. 2011. **24**(5): p. 464-470.
9. Laszlo, E., et al., *Superswelling microneedle arrays for dermal interstitial fluid (prote) omics*. Advanced Functional Materials, 2021. **31**(46): p. 2106061.
10. Kolluru, C., et al., *Recruitment and collection of dermal interstitial fluid using a microneedle patch*. 2019. **8**(3): p. 1801262.
11. Bollella, P., et al., *Microneedle-based biosensor for minimally-invasive lactate detection*. Biosensors and Bioelectronics, 2019. **123**: p. 152-159.
12. Madden, J., et al., *Biosensing in dermal interstitial fluid using microneedle based electrochemical devices*. Sensing and Bio-Sensing Research, 2020. **29**: p. 100348.
13. Kiistala, U. and K.J.J.o.I.D. Mustakallio, *Dermo-epidermal separation with suction: electron microscopic and histochemical study of initial events of blistering on human skin*. 1967. **48**(5): p. 466-477.
14. Saifullah, K.M. and Z.J.A.M.I. Faraji Rad, *Sampling Dermal Interstitial Fluid Using Microneedles: A Review of Recent Developments in Sampling Methods and Microneedle-Based Biosensors*. 2023. **10**(10): p. 2201763.

15. Kool, J., et al., *Suction blister fluid as potential body fluid for biomarker proteins*. 2007. **7**(20): p. 3638-3650.
16. Mitragotri, S. and J.J.A.d.d.r. Kost, *Low-frequency sonophoresis: a review*. 2004. **56**(5): p. 589-601.
17. Park, D., et al., *Sonophoresis in transdermal drug delivery*s. 2014. **54**(1): p. 56-65.
18. Friedel, M., et al., *Opportunities and challenges in the diagnostic utility of dermal interstitial fluid*. 2023: p. 1-15.
19. Nimse, S.B., et al., *Biomarker detection technologies and future directions*. *Analyst*, 2016. **141**(3): p. 740-755.
20. Cao, Z., Y. Jia, and B. Zhu, *BNP and NT-proBNP as diagnostic biomarkers for cardiac dysfunction in both clinical and forensic medicine*. *International journal of molecular sciences*, 2019. **20**(8): p. 1820.
21. Hall, C., *NT-ProBNP: the mechanism behind the marker*. *Journal of cardiac failure*, 2005. **11**(5): p. S81-S83.
22. Lee, H.J., A.W. Wark, and R.M.J.A. Corn, *Microarray methods for protein biomarker detection*. 2008. **133**(8): p. 975-983.
23. Hames, B.D., *Gel electrophoresis of proteins: a practical approach*. Vol. 197. 1998: OUP Oxford.
24. Dunn, M.J., *Gel electrophoresis of proteins*. 2014: Elsevier.
25. Toh, S.Y., et al., *Aptamers as a replacement for antibodies in enzyme-linked immunosorbent assay*. *Biosensors and bioelectronics*, 2015. **64**: p. 392-403.
26. Samper, I.C., et al., *Electrochemical immunoassay for the detection of SARS-CoV-2 nucleocapsid protein in nasopharyngeal samples*. 2022. **94**(11): p. 4712-4719.
27. Warsinke, A., A. Benkert, and F.J.F.j.o.a.c. Scheller, *Electrochemical immunoassays*. 2000. **366**: p. 622-634.
28. Awiaz, G., J. Lin, and A. Wu. *Recent advances of Au@Ag core-shell SERS-based biosensors*. in *Exploration*. 2023. Wiley Online Library.
29. Laing, S., K. Gracie, and K.J.C.S.R. Faulds, *Multiplex in vitro detection using SERS*. 2016. **45**(7): p. 1901-1918.
30. Turner, J.G., et al., *Hydrogel-Forming Microneedles: Current Advancements and Future Trends*. *Macromolecular Bioscience*, 2021. **21**(2): p. 2000307.

31. Sachdeva, V., A.J.R.p.o.d.d. K Banga, and formulation, *Microneedles and their applications*. 2011. **5**(2): p. 95-132.
32. Caffarel-Salvador, E., et al., *Hydrogel-forming microneedle arrays allow detection of drugs and glucose in vivo: potential for use in diagnosis and therapeutic drug monitoring*. 2015. **10**(12): p. e0145644.
33. El-Laboudi, A., et al., *Use of microneedle array devices for continuous glucose monitoring: a review*. 2013. **15**(1): p. 101-115.
34. Lutton, R.E., et al., *Microneedle characterisation: the need for universal acceptance criteria and GMP specifications when moving towards commercialisation*. *Drug delivery and translational research*, 2015. **5**(4): p. 313-331.
35. Aldawood, F.K., A. Andar, and S. Desai, *A comprehensive review of microneedles: Types, materials, processes, characterizations and applications*. *Polymers*, 2021. **13**(16): p. 2815.
36. Li, Q.Y., et al., *A solid polymer microneedle patch pretreatment enhances the permeation of drug molecules into the skin*. 2017. **7**(25): p. 15408-15415.
37. Dharadhar, S., et al., *Microneedles for transdermal drug delivery: a systematic review*. 2019. **45**(2): p. 188-201.
38. Jung, J.H. and S.G.J.J.o.p.i. Jin, *Microneedle for transdermal drug delivery: current trends and fabrication*. 2021: p. 1-15.
39. Yang, J., et al., *Recent advances of microneedles for biomedical applications: drug delivery and beyond*. 2019. **9**(3): p. 469-483.
40. Donnelly, R.F., et al., *Hydrogel-forming microneedle arrays for enhanced transdermal drug delivery*. *Advanced functional materials*, 2012. **22**(23): p. 4879-4890.
41. Oyen, M., *Mechanical characterisation of hydrogel materials*. *International Materials Reviews*, 2014. **59**(1): p. 44-59.
42. Donnelly, R.F., et al., *Hydrogel-forming microneedles prepared from "super swelling" polymers combined with lyophilised wafers for transdermal drug delivery*. 2014. **9**(10): p. e111547.
43. Zheng, M., et al., *Osmosis-powered hydrogel microneedles for microliters of skin interstitial fluid extraction within minutes*. 2020. **9**(10): p. 1901683.

44. He, R., et al., *A hydrogel microneedle patch for point-of-care testing based on skin interstitial fluid*. 2020. **9**(4): p. 1901201.
45. Nagarkar, R., et al., *A review of recent advances in microneedle technology for transdermal drug delivery*. 2020. **59**: p. 101923.
46. Dardano, P., et al., *One-shot fabrication of polymeric hollow microneedles by standard photolithography*. 2021. **13**(4): p. 520.
47. Dabbagh, S.R., et al., *3D-printed microneedles in biomedical applications*. 2021. **24**(1).
48. Tarbox, T.N., et al., *An update on coating/manufacturing techniques of microneedles*. Drug Delivery and Translational Research, 2018. **8**(6): p. 1828-1843.
49. Kim, J.D., et al., *Droplet-born air blowing: Novel dissolving microneedle fabrication*. 2013. **170**(3): p. 430-436.
50. Van Der Maaden, K., W. Jiskoot, and J.J.J.o.c.r. Bouwstra, *Microneedle technologies for (trans) dermal drug and vaccine delivery*. 2012. **161**(2): p. 645-655.
51. Bernadete Riemma Pierre, M. and F.J.C.d.t. Cristina Rossetti, *Microneedle-based drug delivery systems for transdermal route*. 2014. **15**(3): p. 281-291.
52. Mdanda, S., et al., *Recent advances in microneedle platforms for transdermal drug delivery technologies*. 2021. **13**(15): p. 2405.
53. Chen, S., et al., *Temperature-stable boronate gel-based microneedle technology for self-regulated insulin delivery*. 2020. **2**(7): p. 2781-2790.
54. Waghule, T., et al., *Microneedles: A smart approach and increasing potential for transdermal drug delivery system*. 2019. **109**: p. 1249-1258.
55. Babity, S., M. Roohnikan, and D.J.S. Brambilla, *Advances in the design of transdermal microneedles for diagnostic and monitoring applications*. 2018. **14**(49): p. 1803186.
56. Miller, P.R., et al., *Extraction and biomolecular analysis of dermal interstitial fluid collected with hollow microneedles*. 2018. **1**(1): p. 173.
57. Mukerjee, E., et al., *Microneedle array for transdermal biological fluid extraction and in situ analysis*. 2004. **114**(2-3): p. 267-275.
58. Shen, M., J.F. Rusling, and C.K. Dixit, *Site-selective orientated immobilization of antibodies and conjugates for immunodiagnosics development*. Methods, 2017. **116**: p. 95-111.

59. Shakeri, A., et al., *Bio-functionalization of microfluidic platforms made of thermoplastic materials: A review*. *Analytica Chimica Acta*, 2021: p. 339283.
60. Liu, E.Y., S. Jung, and H. Yi, *Improved protein conjugation with uniform, macroporous poly (acrylamide-co-acrylic acid) hydrogel microspheres via EDC/NHS chemistry*. *Langmuir*, 2016. **32**(42): p. 11043-11054.
61. Hua, J., et al., *Preparation and properties of EDC/NHS mediated crosslinking poly (gamma-glutamic acid)/epsilon-polylysine hydrogels*. 2016. **61**: p. 879-892.
62. Wang, C., et al., *Different EDC/NHS activation mechanisms between PAA and PMAA brushes and the following amidation reactions*. *Langmuir*, 2011. **27**(19): p. 12058-12068.

Hypothesis and Research Objectives

Hypothesis

As highlighted in this chapter, microneedles (MNs) have garnered considerable interest not only for their established role in therapeutic delivery but also for their emerging potential for diagnostic applications. Specifically, hydrogel microneedles (HMNs) provide exceptional attributes for gentle extraction of interstitial fluid (ISF) due to their porous structure. Accordingly, our research hypothesis is as follows:

HMNs can be developed for specific detection of protein biomarkers while extracting skin's ISF.

Research Objectives

In order to validate the aforementioned hypothesis, we undertook the following research objectives:

- 1- Fabrication and functionalization of hydrogel square samples (HSSs) with bovine serum albumin (BSA) as a model protein (**Chapter 2**).

This aim was pursued to verify the feasibility of activating the functional groups (COOH) within the hydrogel and establishing bonds between the protein's amine groups and the hydrogel.

- 2- Fabrication and functionalization of HMNs with IgG antibodies to enable the detection of protein biomarkers from the skin within the absorbed ISF (**Chapter 2**).

To achieve this objective, the initial step involved optimizing hydrogel functionalization with IgG antibodies. Then, alteration of hydrogel formulation to provide effective mechanical properties after functionalization.

Chapter 2

As discussed in Chapter 1, microneedles (MNs) offer a safe, painless, and economical method of sample collection. Moreover, they introduce novel prospects for monitoring and diagnostics. This chapter substantiates the potential of hydrogel microneedles (HMNs) for diagnostic applications. Moreover, it illustrates how HMNs can effectively capture biomarkers through hydrogel functionalization with antibodies. This demonstration underscores the valuable potential of HMNs as proficient biomarker capture tools.

Developing Hydrogel Microneedle for Protein Biomarker Detection

Naghme Rezania¹, Xavier Banquy¹, Gregory De Crescenzo², and Davide Brambilla^{1}*

¹Faculté de Pharmacie, Université de Montréal, C.P. 6128, Succursale Centre-ville, Montréal,
Québec, Canada.

²Department of Chemical Engineering Polytechnique Montréal, Montréal, Québec Canada.

*Corresponding author: davide.brambilla@umontreal.ca

2.1. Abstract

The detection of biomarkers plays a critical role in the early identification of diseases and the development of personalised treatment strategies in the field of diagnostics. Hydrogel microneedles (HMNs) have gained recognition as very promising instruments for biomarker detection due to their minimally invasive nature and effective sample capabilities. Notably, the swelling properties of HMNs contribute significantly to the enhancement of these desirable characteristics. The primary aim of this research is to functionalize HMNs with specific antibodies, thereby establishing a proof-of-concept for the detection of protein biomarkers present in the interstitial fluid (ISF) of the skin. The porous nature of HMNs, in conjunction with antibody functionalization, facilitates the extraction of ISF and presents opportunities for disease diagnostics.

Keywords: Diagnosis, labelling, microneedle, interstitial fluid, protein

2.2. Introduction

The potential benefits of biomarkers have been a significant driving force for both academic and industry researchers to employ cutting-edge proteomic technologies in the exploration of biomarkers discovery. Furthermore, there is an increasing demand to establish quantitative analytical techniques that provide rapid and exceptionally sensitive identification of biomarkers [22]. Among a variety of biomarkers, protein biomarkers which are linked to disease progression has attracted immense attention.

Dermal interstitial fluid (ISF) holds significant physiological insights and convenient accessibility yet obtaining it with minimal invasiveness is complex as conventional methods often disrupt its composition through trauma device. ISF shares similarities with serum and plasma in its transcriptome and proteome; this similarity suggests ISF to replace blood for health monitoring. In previous research, they successfully established a correlation between the concentration of a specific protein biomarker in both ISF and plasma [9, 32, 56].

The utilization of MNs for the purpose of extracting ISF has been suggested as a means of conducting minimally invasive monitoring and diagnostic procedures. HMNs excel over alternatives, offering versatile monitoring with self-disabling features and minimal blockage risk. They soften and leave no polymer residue as they're removed with ISF uptake [32, 56].

Antibodies have emerged as the primary choice among the numerous types of capture probe agents utilized for biomarker detection. In 2001, Haab et al. pioneered the effective use of antibody microarrays for high-throughput proteomics. Since then, substantial progress has been achieved in antibody microarray technology, overcoming challenges related to stable, high-density immobilization of antibodies on surfaces while preserving their bioactivity [63-66].

Multiple techniques (click chemistry, EDC/NHS, ...) are available for chemically immobilizing antibodies onto polymeric platforms, each carrying its own set of advantages and disadvantages [63-66]. Developed by Xiaoxuan Zhang et al., flexible MNs loaded with photonic crystal (PhC) barcodes were employed to detect multiple biomarkers, with the barcodes immobilized with antibodies using EDC/NHS. Also, there are some studies which shows the biomolecule immobilization using click chemistry of polymer for different purposes including detection of biomarkers [63, 67, 68].

In this study, by combining the advantages of HMNs as a porous structure for the ISF extraction and antibodies as a detection agent, a novel bio-detection HMNs was developed for specific protein biomarker detection within ISF. After fabrication of HMNs utilizing a pre-established hydrogel formula developed by our group, they were functionalized with antibodies commencing with copper-free click chemistry and transitioning to EDC/NHS chemistry to assess the impact of these distinct approaches on this process. Fluorescence intensity was recorded for both functionalized and control samples, demonstrating the precision of the procedure. Subsequently, the formulation was altered to regulate the swelling ratio of MNs after functionalization, aiming to decrease it. Therefore, after applying the modification on hydrogel formulation, these MNs again underwent antibody functionalization. Mechanical and swelling properties of the MNs were subsequently assessed. The findings indicated the effective antibody functionalization of the hydrogel using EDC/NHS. Moreover, the results demonstrated suitable mechanical properties for skin penetration as well as swelling attributes conducive to ISF absorption. The primary ability of these MNs for the capture and detection of BSA protein biomarker was also examined. However, this part needs more investigation to prove that MNs can capture and detect protein biomarkers.

2.3. Materials and methods

2.3.1. Materials

Cy5-NHS was synthesized by our lab members [69]. Polyacrylic acid (450 kDa), bovine serum albumin (BSA), Dibenzocyclooctyne-N-hydro (DBCO), N-Dimethyleaminopropyl-N ethylcarbodiimide hydrochloride ($M_w=191.7\text{g/mol}$), human serum immunoglobulin (salt free, $\geq 95\%$), anti human IgG (H+L) FITC conjugated (goat polyclonal) were all purchased from Sigma-Aldrich (St. Louis, MO). Bovine albumin polyclonal antibody (Sheep, conjugated with FITC) and bovine albumin polyclonal antibody (rabbit, unconjugated) were purchased from Thermo Fisher. Sodium carbonate (Na_2CO_3) and polyethylene glycol (10 kDa, thermo scientific) were purchased from Thermo Scientific. N-Hydroxysuccinimide (NHS, 98+%) was purchased from Alfa Aesar. 3-azidopropylamine was purchased from Click Chemistry Tools company. Dimethyl sulfoxide (DMSO) was purchased from Acros Organics (Morris Plains, NJ). Sephadex G-50 was purchased from GE Life Sciences (Mississauga, ON). Square pyramidal female MN moulds made of room temperature vulcanizing silicone, 10×10 array, $200 \mu\text{m} \times 200 \mu\text{m} \times 800 \mu\text{m}$ (W \times L \times H) with

peak to peak spacing of 500 μm were purchased from Micropoint Technologies Pte. Ltd. (Singapore).

2.3.2. Characterization

Fluorescence intensity measurements for both HSS and MNs were conducted using a TECAN plate reader at various stages, encompassing functionalization, secondary antibody validation, and post-protein detection. The mechanical properties of MNs were evaluated using a TA.XT-Plus Texture Analyser (Stable Micro Systems, Surrey, UK) in compression mode. The presence of carboxyl (COOH) groups on the hydrogel was assessed utilizing Fourier Transform Infrared spectroscopy (Thermo Scientific Nicolet IS 10, Wisconsin USA). The optical images were taken using fluorescence stereomicroscope (AxioZoom.V16, Zeiss, Oberkochen, Germany) equipped with NIR settings (Excelitas Technologies X-Cite® Xylis light source; Photometrics® Prime™ 95B camera) using a Cy5 filter set ($\lambda_{\text{ex}} = 630 \text{ nm}$, $\lambda_{\text{em}} = 675 \text{ nm}$). Scanning electron microscopy (SEM) was employed for observing the side view of the MNs.

2.3.3. Fabrication of HSSs and MNs

Hydrogel was synthesized using the same formulation developed previously by our group members [9]. In brief, a mixture containing 3% w/w sodium carbonate (Na_2CO_3) and 7.5% w/w PEG was accurately weighed and subsequently transferred into a conical tube; it was then dissolved by adding 5 ml of ultrapure water. The solution was vortexed for 1 min to reach homogenous state. The mixture was completed by addition of polyacrylic acid and 15% w/w Poly (methyl vinyl ether-co-maleic anhydride) (PHVE/ME), respectively. Following the addition of each component, the mixture was vortexed for 1 min. In then next step, the falcons contain aqueous blend of hydrogel formulation were centrifuged for 5 min (4000 rpm, temp 21°C). Then, PDMS molds were placed in 6-wells plate for fabrication of HSSs while 12-well plates were used for MNs. The molds were then entirely filled with the composition and centrifuged at 3000 rpm for 5 min at 21 °C (Sorvall ST 16R, ThermoFisher Scientific, Waltham, MA) to eliminate air bubbles and permit the hydrogel to fully fill the needles. At the end, all the samples were preserved at room temperature for two days to evaporate solvent and one day in the oven (75°C) to crosslink. The samples were obtained by demolding. A head of consume, they were rinsed with a 20% ethanol solution and dried in an oven with the temperature of 40°C.

2.3.4. Labeling of BSA and IgG with Cy5 fluorescence dye

In biochemistry, Cy5 has been applied to label nucleic acids and proteins as a reactive, water-soluble fluorescent dye [70]. The Cy5 stock solution was generated through the dissolution of 3 mg of Cy5-NHS in DMSO, resulting in a concentration of 4.68 mM. The BSA was labeled with a Cy5-NHS fluorescence dye (dye/protein molar ratio: 7). To accomplish this, a solution of BSA was prepared by dissolving 3 mg of BSA in 1.8 ml of PBS adjusted to a pH of 7.4. Afterward, 80 μ l of Cy5 stock solution with a concentration of 4.68 mM was carefully introduced into the mixture while stirring. The resulting mixture was stirred for 4 hours in a dark condition at room temperature (21°C). The separation of free dye from the conjugated protein was achieved through employment of a Sephadex-G50 column. Thin layer chromatography (TLC) was utilized to verify the absence of any free dye after Sephadex column separation process.

IgG was also labeled with Cy5-fluorescent dye. Selecting appropriate buffer was one of the challenges in IgG labeling since protein aggregation could occur during the labeling process and pH could affect the hydrogel's shape throughout hydrogel functionalization. Upon consideration of these two parameters, PBS with a pH of 8.11 was determined as an optimal choice for the labeling. Therefore, 3 mg of IgG was dissolved in PBS by gently shaking with hand, adding 80 μ l of Cy5-NHS solution dropwise to it while stirring; the final solution was stirred for 4 hours in a dark condition. Then, the unbound dye has been isolated from conjugated protein using Sephadex-G50 column, and again TLC was used for analysis. The number of mole dye per mole protein [71] was calculated using the following equation:

$$\text{Equation (1): } \frac{D}{P} = \frac{A_{650}\epsilon_{BSA}}{(A_{280} - 0.05A_{650})\epsilon_{CY5}}$$

Developed by Kaneta Jing et al., in this equation, A_{650} and A_{280} represent the absorbance of labeled protein at 280 nm and 650 nm. The molar extinction of ϵ_{BSA} and ϵ_{CY5} were obtained from references. The number 0.05 shows absorbance of the dye at 280 nm [71].

2.3.5. Functionalization of HSSs with protein molecules (BSA and IgG)

Hydrogels hold significant promise for biomolecule conjugation through mechanisms including physical interactions (non-covalent) or chemical interactions (covalent) [72]. The objective of this study is to investigate the process of biomolecule functionalization of hydrogel through chemical interaction, resulting in the formation of covalent bonds between the functional groups of the hydrogel and specific proteins such as BSA and antibodies.

2.3.5.1. Application of Copper free Click Chemistry

Functionalization was first started by employing copper free click chemistry reaction as it shows more stability and high efficiency in biofunctionalization of polymers and hydrogels. The details of functionalization process are mentioned in the following paragraphs.

2.3.5.1.1. Hydrogel functionalization with BSA using copper free Click Chemistry

Initially, the functionalization process was carried out on the free-needle HSS. To facilitate this, BSA was utilized as a protein model to track the reaction between the COOH groups present in the hydrogel and NH₂ groups of the protein. The click chemistry approach was adopted for this purpose, utilizing two linkers: DBCO-NHS and azido propylamine. EDC, azido propylamine, DBCO-NHS were all prepared with the concentration of 3.8 mM, 3.8 mM, and 1.4 mM, respectively. Two distinct conditions were considered for this functionalization (Figure 2-S1).

In the primary condition, a mixture of EDC (10 μ l) and azido propylamine (27 μ l) was prepared and introduced to the hydrogel. Afterward, the hydrogel was positioned on a plate and then covered with parafilm at ambient temperature, facilitating the activation of COOH groups. Simultaneously, a solution comprising DBCO-NHS (27 μ l) and BSA-Cy5 (15 μ l) was also prepared and incubated for a duration of 1h and 30 min. Next, DBCO-NHS along with BSA-Cy5 was added to the hydrogel, and it was placed in an incubator for 1 h and 45 min (Incubator temperature: 32°C, shaking speed: 65).

Under the second condition, EDC and azidopropylamine were mixed. Additionally, DBCO-NHS was combined with BSA-Cy5 and incubated for 1h and 30 min. Then, the vials containing EDC/azidopropylamine and DBCO-NHS/BSA-Cy5 were combined, and the resulting mixture was added to the hydrogel. The hydrogel was placed in the shaking incubator for 1h and 45 min to

activate COOH groups and bonding amine groups of BSA (Incubator temperature: 32°C, shaking speed: 65).

In both circumstances, the last step was placing the samples in the oven (40°C) for drying. To remove unbounded BSA-Cy5, the samples were rinsed with 20%-ethanol solution three times, and the fluorescence intensity of the samples before washing and after each time washing was recorded.

2.3.5.1.2. Hydrogel functionalization with IgG using Copper free Click Chemistry

In these experiments, the free-needle HSSs were functionalized with IgG-Cy5. The process of functionalization was carried out using the second condition employed in a previous experiment. Accordingly, a mix of linkers was prepared and introduced to the hydrogel samples with similar concentrations and volumes of each component. The samples were incubated for 1h and 40 min. Then, they were dried in an oven (40°C) and rinsed three times with 20%-ethanol solution. Using a TECAN plate reader, the fluorescence intensity before and after each washing step was recorded. The washing process for both the functionalized and control samples was extended to a total number of seven times in order to enhance the differentiation between them based on fluorescence intensity.

2.3.5.1.3. Comparison of hydrogel functionalization with IgG-Cy5 and IgG-FITC

In this experiment, the objective was to examine the impact of two distinct fluorescent dyes on the hydrogel samples. To achieve this, the hydrogel samples were functionalized with IgG-Cy5 (prepared using the previously mentioned method) and IgG-FITC (the labeled version of which was purchased from Sigma Aldrich). Functionalization procedure was fulfilled through the formerly developed method (Second condition). Subsequently, the samples underwent a series of rinses using a 20% ethanol solution, followed by oven drying. This washing and drying procedure was repeated three times. The fluorescence intensity was measured before the initial wash and after each subsequent wash for all the samples.

2.3.5.2. Application of EDC/NHS

The subsequent series of experiments have focused on employing EDC/NHS chemistry to activate COOH groups on hydrogel and bonding to antibodies. Initially, low concentration of EDC and

NHS were used, and then progressed to higher concentration to see how it affects the functionalization process.

2.3.5.2.1. Functionalization of hydrogel with IgG-Cy5 using low concentration of EDC and NHS

At first, experiments were conducted using low concentration (0.06 M) of EDC/NHS. To do this, EDC was dissolved in DMSO (10 mg/ml), and NHS was dissolved in water (20 mg/ml). The hydrogel samples were placed in a 6-wells plate, and a mixture of linkers (20 μ l EDC and 15 μ l NHS) was added to them (Molar ratio EDC/NHS=1). The plate was sealed with parafilm and kept at ambient temperature for a duration of 2 hours. Subsequently, a volume of 35 μ l of IgG-Cy5 was applied onto each hydrogel. The samples were then transferred to a shaking incubator (Temperature= 32°C, shaking speed= 60) for 1h and 30 min. Afterward, the samples were dried in the oven (40° C), and underwent a total of four wash cycles using a 20% ethanol solution, intended to eliminate any unreacted antibodies. Fluorescence intensity measurements were taken both before the washing process and after each individual wash. Control samples were treated differently; the EDC/NHS components were excluded, and just their solvents were introduced in equal proportions to those used for functionalization.

2.3.5.2.2. Functionalization with high concentration of EDC and NHS

This experiment was conducted with a higher concentration (1 M) of EDC and NHS. To estimate the optimal concentration of these reagents for activating all COOH groups on the hydrogel, the number of COOH groups, which represents the required mole of EDC and NHS for this procedure, was calculated. The hydrogel was found to have approximately 0.01 mole of COOH. Considering that each mole of COOH requires a mole of EDC and NHS, 0.01 moles of EDC and NHS are needed to activate all COOH groups on the hydrogel. Thus, 0.01 mole of EDC and NHS (2 g of each) was accurately weighed and subsequently dissolved in 10 ml of water in separate falcon tubes. Specific volume of EDC (1ml) and NHS (1ml) were collected and poured into each well of plate, then hydrogel sample was immersed in each well containing EDC/NHS. The plate was sealed with parafilm and remained at room temperature (21°C) for 30 min to activate COOH groups of the hydrogel. The samples were then removed from the EDC/NHS and transferred to 6 well plates. Next, 150 μ l of IgG-Cy5 (0.01 Mm) was applied to each hydrogel sample and incubated in the fridge (4°C) overnight in darkness. After that the samples were dried in an oven

at 40°C. Next, they were rinsed multiple times with a 20% ethanol solution to remove unreacted antibodies. Fluorescence intensity before washing and after each washing was measured.

The next experiments were performed with the aim of controlling swelling properties of the samples during functionalization. In this regard, the selection of appropriate solvents for EDC and NHS is important as it affect tremendously on hydrogel's swelling ratio. Therefore, the EDC solvent was changed to ethanol instead of water. Functionalization was accomplished using the same method, by immersion of samples in EDC/NHS and then incubation with IgG-Cy5 overnight at 4°C. The samples were then dried in the oven (40°C) and washed three times with 20% ethanol solution. Fluorescence intensity was recorded before and after washing.

In the next experiment, a few changes were made to the procedure to decrease protein absorption specifically on control samples. In this case, the washing steps were carried out immediately after incubation overnight; without a drying step between incubation and washing. The samples were washed two times (each time 5 minutes), and they were all transferred to the oven (40°C) for drying. The fluorescence intensity was measured after drying.

2.3.6. Validation of the functionalization using fluorescent labeled sABs

To verify functionalization, fluorescent labeled sABs was utilized. To do this, the samples were first functionalized with IgG using the procedure described above. After doing all the steps and drying the samples, they were incubated with 150 µl of anti human IgG (H+L)- FITC (goat polyclonal, 0.5 mg/ml) overnight at 4°C to bind the sABs to pABs. Then, they were washed two times with 20% ethanol solution directly after incubation overnight with the aim of removing unbounded antibodies; then they were dried at 40°C. The fluorescence intensity was measured using TECAN plate reader.

2.3.7. Modifying hydrogel formulation

In all previous functionalization, square samples of the free-needle hydrogel were employed, yielding positive results. When it came to functionalization of hydrogel MNs (HMNs), the samples were unable to withstand the functionalization process and subsequent washing steps, and majority of them lost their original shape because of over swelling. Consequently, it was decided to control the swelling properties of hydrogel by decreasing the amount of sodium carbonate. Thus, in

modified formulation, the quantity of sodium carbonate has been reduced from 0.220 gr to 0.110 gr. In the same way as the first formulation, the synthesis process was initiated by accurately measuring Na_2CO_3 and PEG. Subsequently, the measured quantities were transferred to a Falcon tube and dissolved in 5 ml of ultrapure water and vortexed for 1 min. The formulation was then completed by adding polyacrylic acid and Gantrez S-97, respectively. Following the addition of each component, the mixture was vortexed for 1 min. Then, the falcons were centrifuged (5 minutes, temperature 21°C, 4000 rpm) to spin down the formulation. The MNs molds were placed in plates (6-wells plate for the square molds and 12-wells plate for the MNs molds). After filling the molds with the formulation, they were centrifuged to remove unwanted bubbles and fill in any gaps. Then, the molds containing hydrogel formulation were removed from the plate and left at room temperature (21°C) for one day, followed by two days in an oven (75°C). The samples were then washed for 30 min to remove unbound crosslinkers and reagents, and then dried in an oven (40°C). Finally, they were maintained in a desiccator.

2.3.7.1. Functionalization of modified hydrogel formulation (MHF) with IgG-Cy5 using EDC/NHS at high concentration

Functionalization was successfully carried out through the current developed procedure involving the preparation of EDC/NHS solutions with higher concentrations. The samples were then immersed in a mixture of EDC/NHS for 30 min at room temperature (21°C) in order to activate COOH groups. Accordingly, the samples were taken out of the solution and transferred to another plate; subsequently, 150 μl of IgG-Cy5 (0.01 mM) was administered to each sample, followed by an overnight incubation at 4°C. Following this, the samples were rinsed three times with 20% ethanol washing solution to remove any unbound IgG-Cy5. They were then dried in an oven (40°C). Fluorescence intensity of the samples was recorded after drying.

2.3.8. Validation of functionalization using sABs

The samples underwent initial functionalization with IgG, and as in previous steps, they were subsequently washed and dried. After that, 150 μl of IgG-FITC (0.5 mg/ml, labeled secondary antibody) was added to each sample, and they were incubated overnight in the fridge, enabling the secondary antibody to bind with the primary antibody. Right after the incubation period and prior to the drying process, the samples underwent two consecutive rinses with a 20% ethanol solution.

This step was taken to eliminate any sABs that hadn't bound to the samples. After the samples had been thoroughly dried, the fluorescence intensities of each sample were measured.

2.3.9. Mechanical properties of hydrogel

The mechanical resistance of hydrogel MNs is a crucial characteristic as MNs experience various stresses including the forces during administration to different parts of the skin, inevitable motions during insertion and the pressure applied during removal process. The appropriate mechanical properties lead to efficient application of MNs in the processes of skin penetration, transdermal delivery of therapeutic substances, and extraction of biological fluids. Not only it should be strong, but also it should have enough elasticity to avoid breakage prior to skin penetration. The mechanical properties of MNs were evaluated using a TA. XT-Plus Texture Analyser (Stable Micro Systems, Surrey, UK) in compression mode. Simply, the MNs' backing layer was affixed to the metal base, with the needles oriented upward. The cylindrical stainless-steel probe (6 mm diameter) was moved towards the needles in vertical direction at a speed of 5 mm s⁻¹ and compress it for a distance of 0.3 mm for 10 seconds before returning to its original position at a speed of 10 mm/s. The maximum tolerable force by the MNs was determined according to maximum of the force-time curve. The setting parameters were determined through a combination of insights from prior studies and our own observations, achieved by experimenting with various parameters. The mechanical characteristics of HMNs, produced through the modified formulation, were assessed both prior to and following functionalization.

2.3.10. Swelling ratio of hydrogel MNs

The swelling ratio serves as an indicator of the hydrogel's capacity for water absorption. Here, the swelling ratio of modified-formulation hydrogel samples was measured both prior to and following the functionalization process. To evaluate the swelling ratio of both groups, they were submerged in 3 ml of ultrapure water for varying time durations (5, 10, 15, 20, 30, 60, 90, 150, 240, 330, and 420 min). Prior to immersion, the samples were weighed (W₀) to establish an initial value. After a specified time period, the swollen MNs were removed from the water, and any excess surface water was removed using tissue paper. The weight of the hydrogel in its swollen state was

measured subsequent to the removal of the solution [73]. The following equation was used to report the swelling ratio percentage of the samples:

$$\text{Equation (2): \% Swelling ratio} = \left[\frac{W_s - W_0}{W_0} \right] \times 100$$

2.3.11. Capture protein biomarker using HMNs

In order to assess the MNs capability for detecting protein biomarkers, BSA was chosen as the protein biomarker for this experiment. To achieve this objective, the HMNs were initially modified by functionalizing them with anti-BSA polyclonal rabbit antibodies (200µg/ml) following the previously optimized protocol. The samples were ready for capture after being washed and dried. Subsequently, various quantities of BSA solutions were produced, specifically 0, 10, 20, 30, and 40 µg/ml. Each sample was submerged in a 600 µl of BSA solution for a duration of 2 hours at 4°C. Afterwards, the samples underwent a single washing procedure using a 20% ethanol solution for a duration of 5 minutes. Right after this phase, the samples were subjected to the addition of anti-BSA polyclonal sheep antibody (200 µg/ml), which had been conjugated with FITC and served as the secondary antibody. The samples were then left to incubate overnight at 4°C. Next, the samples underwent two rounds of rinsing using a 20% ethanol solution and dried in oven (40°C). The fluorescence intensity of the samples was measured and recorded.

2.4. Results and discussion

2.4.1. Synthesis of hydrogel free-needle samples and HMNs

HMNs possess certain advantages over other MNs owing to their potential for ISF collection and biomarkers detection. Laszlo et al. developed a superabsorbent HMNs capable of ISF extraction by penetration to the skin [9]. Using the same formulation, acrylic acid hydrogel samples were obtained by thermal crosslinking in the presence of PEG (Figure 1(A)). This formulation benefits from the combination of PHVE/ME (Gantrez S-97) and polyacrylic acid features. According to numerous studies, Gantrez S-97 has been identified as a suitable polymer for HMNs due to its favourable swelling properties and ability to form a 3D crosslinked network of hydrogel [74-76]. On the other side, polyacrylic acid displays multiple advantageous properties, including water solubility, biocompatibility, and non-toxicity. Additionally, it has the ability to undergo

crosslinking, resulting in the formation of a stable structure that is highly suitable for hydrogel fabrication [77, 78]. Therefore, inclusion of polyacrylic acid not only enhance the swelling properties of hydrogel but also lead to existence of more COOH clusters on the crosslinked hydrogel which is favourable for the biofunctionalization [79]. The COOH groups on the crosslinked hydrogel colored in red in figure 2-1(A) are the favourable sites for biomolecules bonding such as antibodies, protein, etc.

Table 1. FTIR peaks correspond to synthesized hydrogel.

Bond	Peaks
C=O stretch	1760-1690 cm^{-1}
C-O stretch	1320-1210 cm^{-1}
O-H bend	1440-1395 cm^{-1} , 950-910 cm^{-1}
O-H stretch	3300-2500 cm^{-1}

Figure 2-1(B) displays the FTIR analysis of the crosslinked hydrogel, revealing distinct peaks that correspond to the presence of unbound COOH groups within the hydrogel. The observed peaks within the spectral range of 3300-2500 cm^{-1} and 1760-1690 cm^{-1} can be attributed to the stretching vibrations of the O-H bond and the C=O bond, respectively. Furthermore, it can be observed that the peak in the spectral range of 1320-1210 cm^{-1} is associated with the stretching vibration of C-O bond. The peaks in the range of 1440-1395 cm^{-1} and 950-910 cm^{-1} indicates the presence of an O-H bend (Table 1).

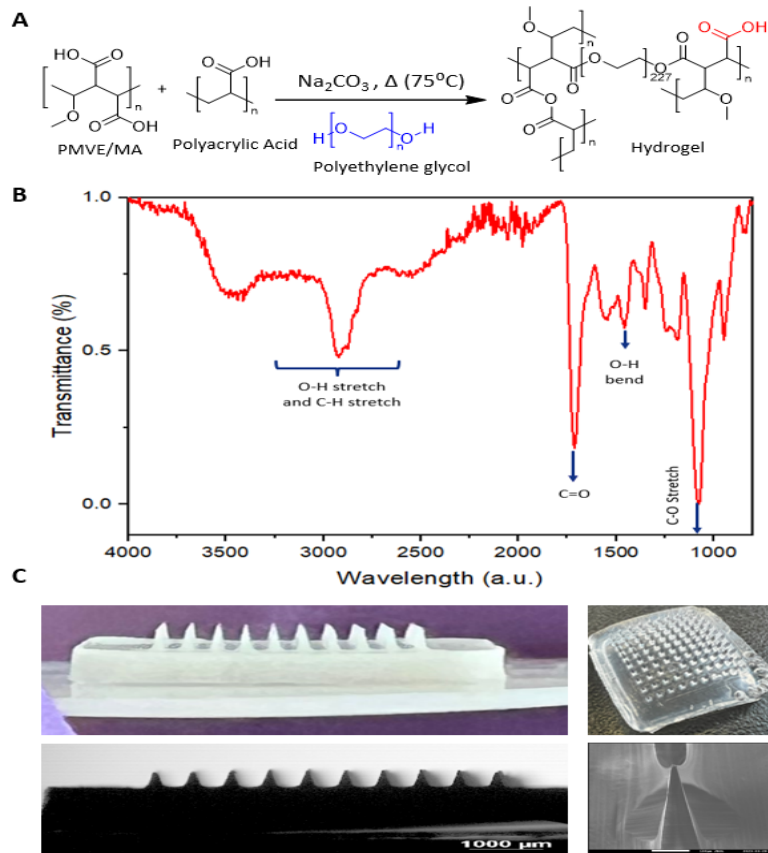


Figure 2-1. Hydrogel formulation and samples shape: (A) Hydrogels synthesis formulation. (B) FTIR of synthesized hydrogel. (C) Image of MNs shape including the images taken by conventional camera (upper left and right side) and microscopic images (lower left side), and SEM images (lower right side).

In Figure 2-1 (C), the morphology of microneedles (MNs) is illustrated through conventional camera, microscopic, and SEM imaging techniques after the fabrication process. The upper left image displays a side view of the microneedle captured with a conventional camera, while the lower left image shows the side view taken with a microscope. Both images reveal a neatly organized row of microneedles, each exhibiting a sharp pyramid shape. The right side of the figure includes an overview of the microneedles at the top, and in the lower corner, there is a magnified SEM image of a single needle. Based on these images, it is evident that the MNs have a pronounced pyramid-like shape, gradually narrowing from a broader base to a fine, needle-like tip. All the needles were fully formed and possessed sufficient sharpness for effective skin penetration.

2.4.2. Labeling of BSA and IgG with Cy5 fluorescence dye

BSA is an abundant and easily accessible protein with a wide range of biochemical properties. It is used in medical, pharmacological, and biochemical applications, including enzyme catalysis, immunoassays, and protein structure studies [80]. As a protein model, BSA was used to determine the reaction between its amine groups and the COOH groups of the hydrogel. To track the reaction, BSA was labeled with Cy5-NHS fluorescence dye. Cy5-NHS is a widely utilised fluorescent dye employed for protein labelling in diverse biological and biochemical applications. This compound belongs to the cyanine dye family and is renowned for its vivid red fluorescence. Cy5-NHS is frequently employed in fluorescence-based imaging, flow cytometry, protein quantification, and a range of other molecular biology methodologies. The presence of NHS ester moiety in Cy5-NHS facilitates its interaction with primary amines ($-NH_2$) present in proteins, peptides, or other compounds, leading to the creation of a durable covalent linkage [81]. The NHS ester, which is amine-reactive, exhibits a high reactivity towards primary amines within a pH range of 7-9, making it suitable for use in various biological systems [82].

BSA protein was effectively conjugated with Cy5-NHS, and no evidence of protein aggregation was detected subsequent to the labeling process. However, IgG labeling was challenging due to the possibility of protein aggregation and hydrogel shape changes by using improper buffer. A variety of buffers, including sodium bicarbonate buffer (pH=9.7), and PBS buffer (pH=6, 7.4, 8.11), were used for IgG labeling, following the same procedure as for BSA labeling. Although sodium bicarbonate did not cause protein aggregation during the labeling process, it tremendously affected the hydrogel shape and obtained unfavourable results. Alternatively, PBS buffer (pH=6, 7.4) shows compatibility with hydrogel samples, but causes protein aggregation after labeling. Therefore, PBS buffer with the pH=8.11 was finally selected for the IgG labeling as it showed no sign of protein aggregation, and it did not affect hydrogel shape. To separate IgG-Cy5 from free dyes, gel filtration chromatography using Sephadex G-50 was used. Sephadex is a frequently employed gel filtration technique that is utilised for the purposes of purifying, exchanging buffers, and fractionating biomolecules, primarily relying on the principle of size exclusion. The TLC confirmed the accuracy of separation by showing negligible free dye in labeled IgG.

In order to investigate the impact of labeling on Cy5, the excitation and emission spectra of BSA-Cy5 and IgG-Cy5 were compared to that of Cy5 (Figure 2-2). The tagged IgG and BSA had

excitation (at 651 nm) and emission (670 nm) peaks that were identical to Cy5. As a result, labeling had no effect on the excitation and emission spectra of Cy5. The number of dye mole/protein mole for BSA-Cy5 and IgG-Cy5 was 1.6 and 3.4, respectively.

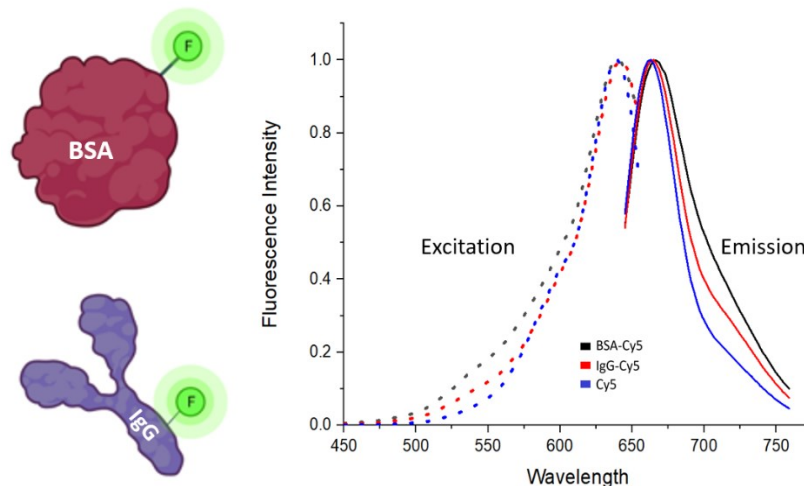


Figure 2-2. Cy5 excitation and emission; Spectrums of Cy5, BSA-Cy5, and IgG-Cy5.

2.4.3. Functionalization of hydrogel using copper-free click chemistry

Hydrogels hold significant promise for biomolecule conjugation through mechanisms including physical interactions (non-covalent) or chemical interactions (covalent) [72]. Biofunctionalization using physical interaction offers a smoother approach compared to chemical interactions. In particular, it is straightforward for larger biomolecules like natural polymers, enzymes, and growth factors to conjugate through physical attachment; however, they tend to exhibit inherent instability during *in vitro* analysis or when used for specific applications. Recent advancements in chemical interaction techniques lead to precise orientation of conjugated biomolecules on polymeric surfaces, which is essential for their specialized functionality, such as antibodies and enzymes. Multiple techniques (click chemistry, EDC/NHS, ...) are available for chemically immobilizing antibodies onto polymeric platforms, each carrying its own set of advantages and disadvantages [63-66].

Copper-free click chemistry is an alternative way to traditional copper-catalyzed click chemistry, offering several advantages in various applications specifically in biological and biomedical applications. Unlike copper-catalyzed reactions, copper-free click chemistry utilizes bioorthogonal reactions that do not rely on copper ions as catalysts. [63-66]. In this study, DBCO-NHS and

azidopropylamine were both selected for the biofunctionalization of hydrogel. Figure 2-3(A) illustrates the comprehensive process of hydrogel functionalization with protein biomolecules, encompassing three primary steps: 1) Functionalizing DBCO-NHS with BSA-Cy5 on one end, 2) The activation of the hydrogel's COOH groups through EDC/Azido propylamine, and 3) The bonding of the protein's NH₂ groups to the activated COOH groups. Therefore, the hydrogel samples were functionalized with BSA-Cy5 considering two various conditions mentioned before. In a first condition, functionalization was performed by following these steps: initially, COOH groups were activated by employing a combination of EDC and azidopropylamine. Subsequently, DBCO-BSA-Cy5 was added to covalently bond BSA-Cy5 to activated COOH groups. In a second condition, a mixture of EDC/azidopropylamine was prepared. Subsequently, DBCO-BSA-Cy5 was combined with this mixture and introduced to the hydrogel, leading to the activation of COOH groups and the spontaneous bonding of proteins. Following functionalization with BSA-Cy5, fluorescence intensities of all samples were measured (Figure 2-3 (B)). According to the provided diagram, it is evident that the functionalized samples exhibit a greater fluorescence intensity in comparison to the control. This observation strongly suggests the successful bonding of BSA-Cy5 to the hydrogel samples. Furthermore, the samples that were functionalized with the second condition exhibited a greater fluorescence intensity compared to those functionalized with the first condition. Consequently, the subsequent experimental procedures were conducted using the second condition, which involved the utilization of a mixture of linkers.

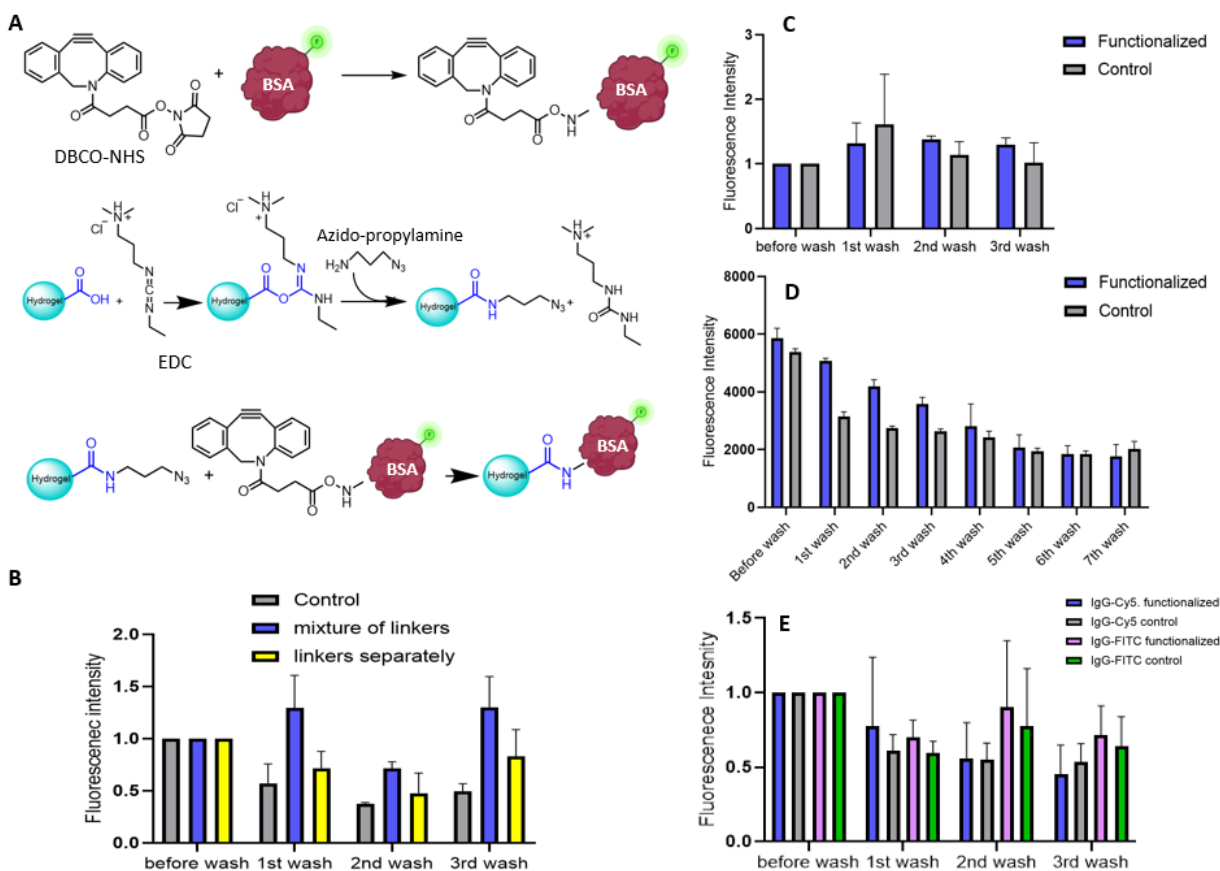


Figure 2-3. Functionalization of hydrogel using copper free click chemistry: A) Schematic of hydrogel functionalization with protein applying copper-free click chemistry. B) fluorescence intensity of functionalized and control samples with BSA-Cy5 using click chemistry reaction. C) fluorescence intensity of functionalized and control samples with IgG-Cy5 using click chemistry reaction after three times washing. D) fluorescence intensity of functionalized and control samples with IgG-Cy5 using click chemistry reaction after seven times washing. E) fluorescence intensity of functionalized samples with IgG-Cy5 and IgG-FITC using click chemistry reaction.

Following the successful functionalization of hydrogel with BSA-Cy5, the experiment focused on the functionalization of hydrogel with IgG-Cy5. To enable functionalization of the samples with IgG-Cy5, the second condition from the previous experiment was implemented. Then the samples were subjected to rinse for three times using a 20% ethanol solution. The fluorescence intensity of the samples was measured before and after washing steps (Figure 2-3 (C)). The findings display a decrease in fluorescence intensity in both the functionalized and control groups after washing process, indicating the removal of the protein. It is anticipated that a significant proportion of the

protein will bind to the hydrogel in functionalized samples, resulting in a noticeable distinction when compared to the control. Nevertheless, no significant difference was observed between the functionalized and control samples. To evaluate the impact of additional washing steps on the fluorescence intensity of both functionalized and control samples, the number of washing steps was increased from three to seven (Figure 2-3 (D)). Based on the results, functionalized and control samples showed adjacent fluorescence intensity after each washing, indicating no considerable difference between the functionalized and control samples. Therefore, it appears that the number of washing steps is not the determining factor, and it should be focused on other parameters. The subsequent experiment aimed to evaluate the impact of employing a different fluorescence dye on the functionalization process. Hydrogel samples were simultaneously functionalized with IgG-FITC and IgG-Cy5 under identical condition. Based on results (Figure 2-3 (E)), no significant difference was observed between the functionalized and control samples in both groups. Moreover, the samples functionalized with IgG-Cy5 and IgG-FITC demonstrated analogous fluorescence intensity. This suggests that the utilization of different fluorescence dyes and labeling processes did not have an impact on the functionalization process. Consequently, a decision was made to investigate an alternative chemical reaction in order to assess its impact on the functionalization process.

2.4.4. Functionalization of hydrogel with IgG using EDC/NHS chemistry

All the former experiments aimed at functionalizing the hydrogel utilized click chemistry reaction, which yielded favorable results for the functionalization of the hydrogel with BSA-Cy5. However, this chemistry did not yield satisfactory results for the functionalization of the hydrogel with IgG-Cy5, despite implementing various changes and modifications. Hence, the subsequent experiments were conducted by utilizing EDC/NHS. The utilization of carbodiimide chemistry represents a prevalent approach for the covalent modification of free carboxylic acids with primary amine groups, serving the purposes of labeling and surface functionalization in laboratory settings. The EDC reagent facilitates the activation of the unreacted carboxyl groups on one molecule, enabling them to form amide bonds with the primary amine groups present on the other molecule. NHS inclusion in EDC reactions is a common strategy due to the considerably higher stability of the intermediate produced by NHS compared to the O-acylisourea formed in reactions involving only EDC [61, 83]. The reaction formula for functionalizing hydrogel with IgG-Cy5 using

EDC/NHS, which consists of two major phases, is shown in figure 2-4 (A). The initial step involves the activation of carboxyl (COOH) groups on the hydrogel using EDC, followed by the inclusion of NHS to form a stable product. The second row is about bonding of NH₂ groups of proteins to activated-COOH groups. This figure also depicts the FTIR spectra of hydrogel, COOH-activated hydrogel, and functionalized hydrogel.

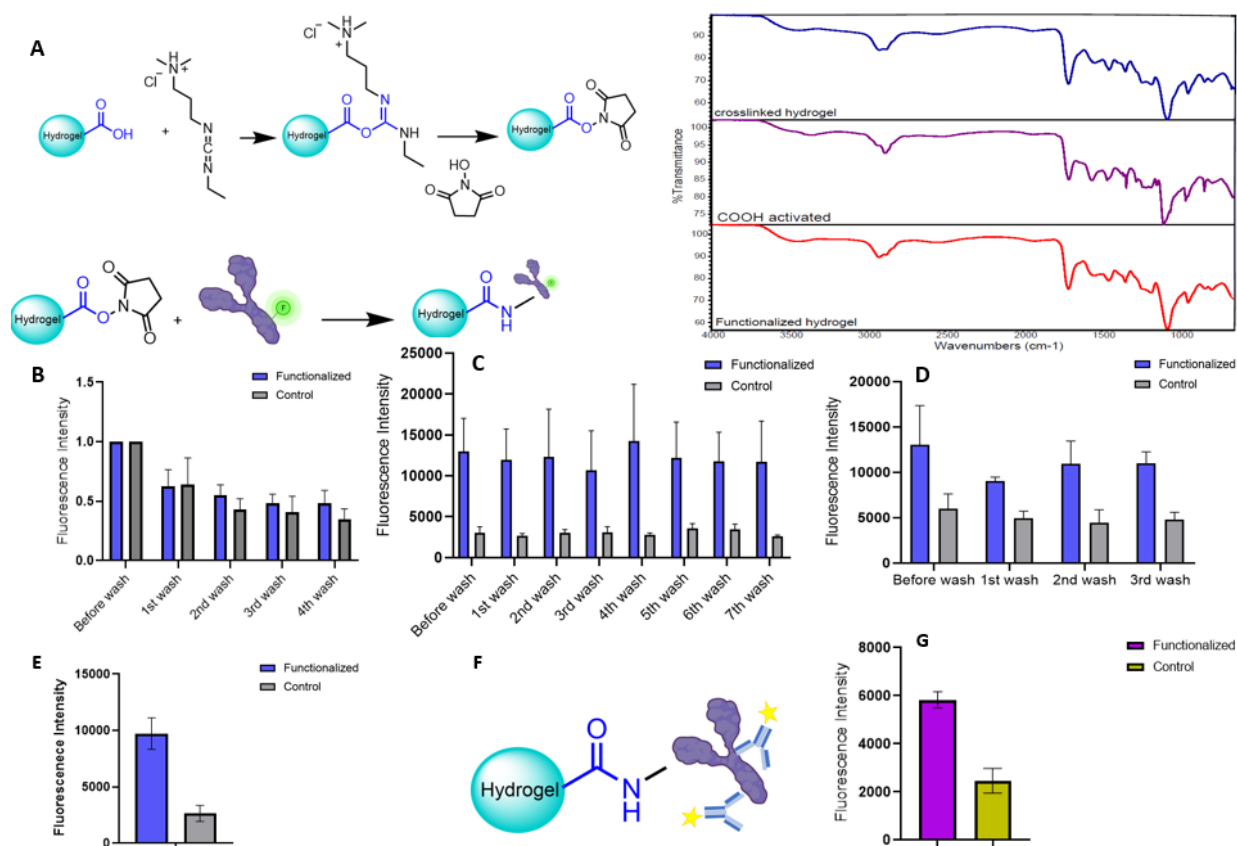


Figure 2-4. Functionalization of hydrogel using EDC/NHS: A) Chemical formula of hydrogel functionalization including COOH activation and bonding of protein. Also, it depicts the FTIR spectrums of synthesized hydrogel, COOH activated hydrogel and functionalized hydrogel. B) Fluorescence intensity of functionalized and control samples using lower mole of EDC/NHS. C) fluorescence intensity of functionalized and control samples using higher mole of EDC/NHS (EDC and NHS solvent: water). D) Fluorescence intensity of functionalized and control samples using higher mole of EDC/NHS (EDC solvent: ethanol, NHS solvent: water). E) fluorescence intensity of functionalized and control samples using higher mole of EDC/NHS (EDC solvent: ethanol, NHS solvent: water) and immediate washing after functionalization. F,G) validation of functionalization using FITC-labeled secondary antibody.

The functionalization process began by immersing the samples in a low-concentrated EDC/NHS solution (0.06 M) to activate the COOH groups. Following that, the samples were subjected to an overnight incubation with IgG-Cy5 in a fridge. This duration allowed for the bonding to occur between the activated carboxyl (COOH) and amino (NH₂) groups. The fluorescence intensity of all samples was measured after undergoing four cycles of washing. The fluorescence intensity indicates that there is no statistically significant difference observed between the functionalized and control samples. Additionally, it is observed that the fluorescence intensity decreases in both groups after each washing (Figure 4 (B)). This decline in fluorescence intensity means that the proteins are washed out from the functionalized sample; and that is the reason for showing similar fluorescence intensity to the control.

There was uncertainty raised regarding whether the quantity of EDC/NHS is adequate to activate all the COOH groups on the hydrogel. To address this issue, the decision was made to investigate the impact of higher concentrations of EDC and NHS on the activation and functionalization of COOH groups. To utilize the optimal concentration of these reagents for activating all COOH groups on the hydrogel, the number of COOH groups, which represents the required mole of EDC and NHS for this procedure, was calculated. Accordingly, high concentrated solution of EDC and NHS (1 M) were prepared, and functionalization was performed. Afterward, the samples were subjected to seven rounds of washing, and the fluorescence intensity was measured before washing and after each subsequent washing cycle. The acquired results showed a significant difference between the functionalized and control samples, demonstrating the efficiency of the functionalization process. As expected, the fluorescence intensity of control samples was 352% lower than that of functionalized samples after 7 times washing since the COOH groups on their hydrogel were not activated. Thus, it was found that EDC/NHS with a concentration of 1 M could activate the majority of the COOH groups on the hydrogel for IgG bonding (Figure 4(C)). The experiment encountered a significant issue with hydrogel over-swelling, despite the successful functionalization with IgG. Choosing the right solvent for EDC and NHS incredibly influences the swelling behavior of the hydrogel. The use of water as the solvent for both EDC and NHS resulted in excessive swelling of the samples. Consequently, in the next experiments, ethanol was employed as a replacement solvent for dissolving EDC, while NHS solvent remained unchanged. The functionalization of the samples was carried out using the identical procedure as before. The observation showed that water and ethanol were found to be the most effective solvents for EDC

and NHS, respectively, in terms of hydrogel swelling during functionalization; this means that the final shape of the hydrogel can be more precisely controlled by mixing water and ethanol. The finding (Figure 4(D)) reveals that the functionalized samples showed 129% higher fluorescence intensity compared to the control samples. However, it is worth noting that the difference between the fluorescence intensity in functionalized and control samples is not as pronounced as observed in previous experiments as clarified by the provided percentage differences in each condition. The rationale for this observation is that the hydrogel in the preceding experiment undergoes more pronounced swelling; therefore, the likelihood of IgG-Cy5 binding to the hydrogel increases, resulting in a corresponding increase in fluorescence intensity.

In order to simplify functionalization process and reduce the number of proteins adsorbed in both samples, the washing steps were rearranged to occur after the overnight incubation and prior to placing the samples in the oven. To remove any unbound IgG-Cy5, the samples were subjected to two rounds of washing with a 20% ethanol solution, with each wash lasting 5 min. Evidently, the control samples displayed 268% lower fluorescence intensity compared to the functionalized samples, indicating a reduction in the number of adsorbed proteins (Figure 4(G)). 73%

2.4.5. Validating the functionalization using labeled secondary antibody

In the context of immunoassays, pABs refer to the antibodies that directly bind to a specific antigen. On the other hand, sABs have the ability to bind to epitopes of the antigen that are different from those utilized for binding with the pABs. In immunoassays, sABs play a valuable role as they are typically conjugated or labeled with enzymes. They are employed as detection antibodies to assess the level of antigen binding to the pABs [19].

In this experiment, following the functionalization of the samples with IgG as the pABs, FITC-labeled sABs were applied and left to incubate overnight at 4°C. To eliminate any unbound sABs, the samples underwent two rounds of washing. Subsequently, the fluorescence intensity of all the samples was recorded after drying. The results demonstrated that the fluorescence intensity of the functionalized samples was 135% more than control samples, indicating the presence of a greater quantity of pABs on the hydrogel compared to the control. The presumption is that sABs will adhere to pABs. This implies that an increase in fluorescence indicates a greater quantity of pABs

attached to the hydrogel. This result confirms the successful and accurate functionalization process.

2.4.6. Characterization of MHF samples

All prior experiments were conducted using free-needle HSSs. However, when attempting to functionalize the MNs, they proved unable to withstand the functionalization and washing steps. This was primarily due to excessive swelling, resulting in the MNs losing their initial shape after drying. Hence, it was determined that modifications are necessary in the synthesis formulation of the hydrogel to regulate its swelling properties. One of the key components in the hydrogel formulation, sodium carbonate, was found to have a remarkable impact on its swelling characteristics. According to existing literature, the hydrogel formulation that incorporated Na_2CO_3 as a modifying agent exhibited enhanced initial swelling and achieved equilibrium at a faster rate compared to the control formula [42]. The reason is that foaming agents increase the void volume, thereby decreasing the density of the hydrogel and causing greater enlargement than hydrogels without foaming agents [84].

MNs were fabricated using the MHF by reducing the quantity of sodium carbonate to half of its original amount. The samples underwent a 30 min washing procedure to remove any unbound crosslinkers. Interestingly, the washing process had no impact on the shape of the hydrogel, as the samples retained their shape even after extended washing durations, which is highly advantageous.

In Figure 2-5 (A), the hydrogel is depicted after the washing process. The microscopy image reveals that the needles exhibit a satisfactory shape, remaining sharp, and their length falls within the range of $668 \pm 27 \mu\text{m}$. The key highlight is that despite the swelling, the MNs return to their original shape without any bending, ensuring that their functionality for skin penetration remains unaffected. Therefore, the modified formulation was chosen for functionalization due to its ability to withstand the washing steps without experiencing any damage.

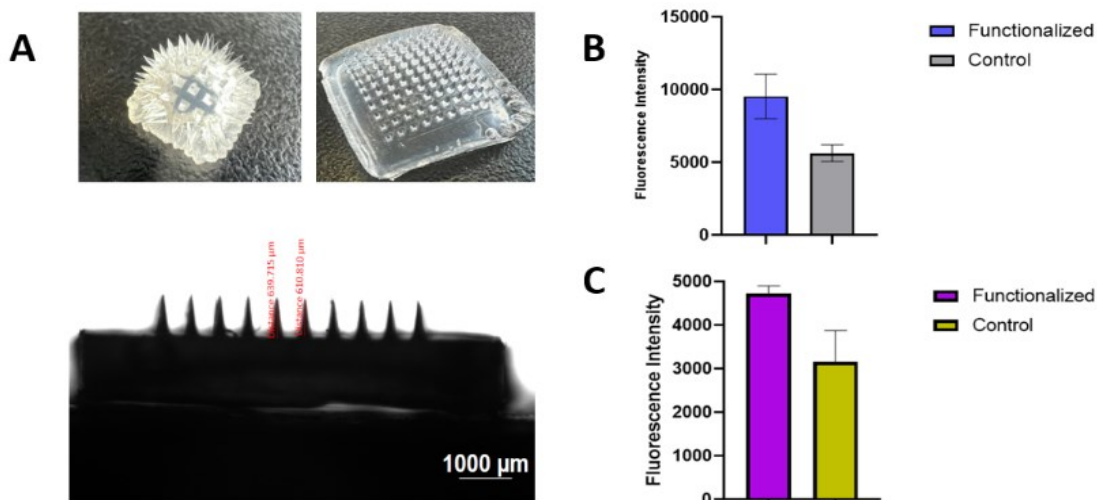


Figure 2-5. Morphology and functionalization of MHF samples: (A) Photographs and microscopic images of MNs using MHF. (B) Fluorescence intensity of functionalized and control samples on modified-formulation hydrogel MNs. (C) Validation of functionalization using labeled secondary antibody on MHF.

2.4.7. Functionalization of MHF samples

Following the synthesis of the hydrogel, the samples underwent functionalization with antibodies using the recently developed procedure. The samples were activated with 1M EDC/NHS solution to activate COOH groups. Subsequently, they were incubated with antibodies overnight at 4°C. The measured fluorescence intensity after drying of the samples show that functionalized samples demonstrate 70% higher fluorescence intensity compared to the control samples, thereby confirming the successful functionalization of the hydrogel with antibodies (figure 2-5 (B)). The current hydrogel exhibits reduced swelling compared to the previous one, and this can be attributed to the decrease in hydrogel porosity resulting from the reduction in the amount of sodium carbonate. In this hydrogel, a lower swelling ratio was observed, which implies a reduced probe immobilization compared to the original hydrogel formulation. Consequently, there is a smaller surface area available for antibody immobilization. These characteristics provide a clear explanation for the significantly higher fluorescence intensity observed in the previous hydrogel samples compared to the modified formulation [32].

2.4.7.1. Validation of functionalization with secondary antibody

To validate the functionalization, FITC-labeled sABs were employed. Again, the hydrogel samples were functionalized with IgG. Subsequently, they were incubated overnight with the sABs, followed by a washing step to eliminate any unbound antibodies. After drying, the fluorescence intensity of the samples was measured. The results indicate that the fluorescence intensity of the functionalized samples exceeds that of the control samples, reflecting the quantity of pABs successfully functionalized onto the hydrogel samples compared to the control (Figure 2-5(C)). Consequently, modifying the hydrogel formulation did not impact the functionalization process. Just a reduction in the quantity of available pores for functionalization, resulted in less antibodies bonding and showing lower fluorescence intensity compared to previous formulation.

2.4.8. Mechanical properties of hydrogel

The efficacy of MNs in skin penetration is significantly influenced by their mechanical properties. These properties are pivotal as MNs must exhibit adequate strength to breach the stratum corneum, all the while maintaining a degree of elasticity to avoid fracturing before penetrating the skin [54]. In contrast to the primary formulation, the modified formulation is anticipated to yield heightened mechanical strength for skin penetration. This improvement is attributed to the reduction in the number of porosities achieved by decreasing the quantity of Na_2CO_3 in the modified formulation. Figure 2-6 (A) shows the mechanical characteristics of the MNs. Based on the diagram, it is evident that both the functionalized and non-functionalized MNs exhibited a maximum tolerable force of approximately 3 N. This finding underscores the promising capability of MNs for effective skin penetration. As corroborated by existing literature, the acceptable force range for MNs typically falls between 0.1 to 3 N per individual needle over a compression distance of 0.5 mm [85]. Taking into account this description, the MNs demonstrated commendable mechanical attributes. While the functionalized samples exhibited slightly diminished mechanical properties, the distinction is not substantial [86]. Activation with EDC/NHS effectively lowered the energy barrier for carboxyl groups to engage with amine groups. This interaction had the potential to generate urea derivative byproducts like ammonia [61]. The presence of ammonia will cause bubbles to appear in hydrogels, weakening their mechanical properties.

2.4.9. Swelling properties of hydrogel

Swelling of hydrogels refers to their capacity to absorb and retain water, influencing both their dimensions and characteristics. To assess the swelling ratio of MNs over different time intervals, the process involved initially weighing the samples in their dry state, followed by subsequent weighing after immersion in water for various time durations. The percentage swelling ratio was computed using equation (2). The outcomes indicate that the functionalization process had a limited impact on altering the swelling properties of the HMNs. As depicted in the figure 2-6 (B), for both functionalized and non-functionalized samples, the swelling ratio experiences an increment from the 5 min immersion to the 30 min immersion. This increase is attributed to the available space for water molecules. However, after an immersion duration of 60 min, the swelling ratio levels off, reaching a plateau region. This feature suggests that the MNs have the capacity for rapid ISF absorption within a brief timeframe. Furthermore, even when the MNs are left in the skin for an extended period, there is no likelihood of experiencing excessive swelling that could potentially result in deformation.

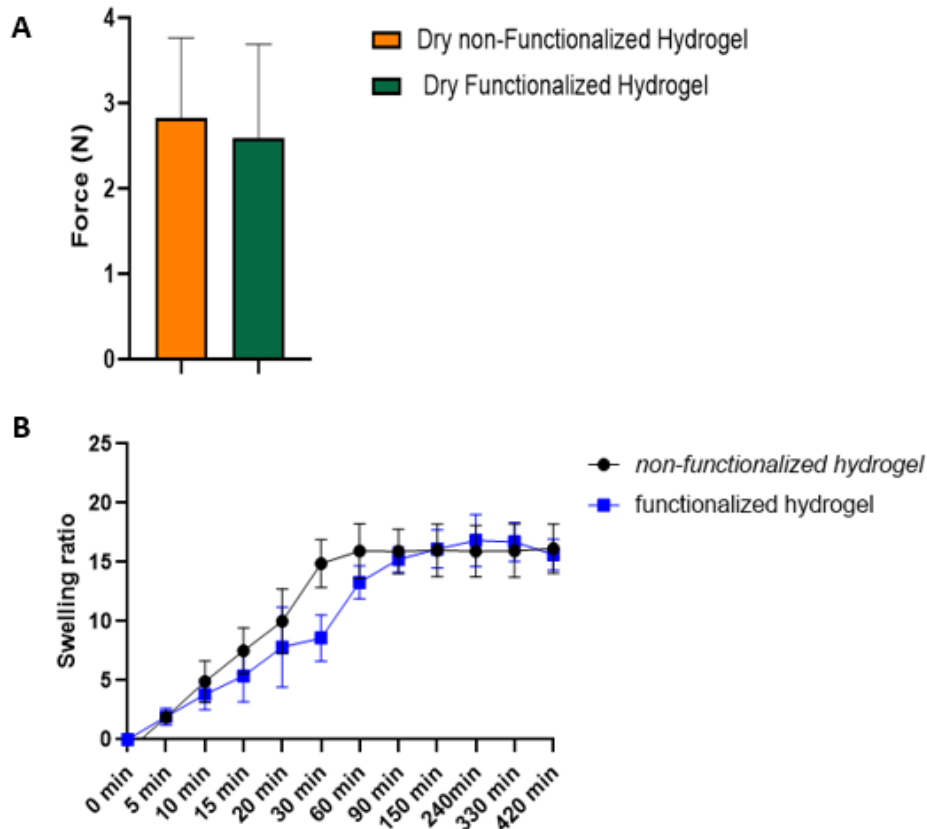


Figure 2-6. Characterization of MHF samples: (A) Mechanical properties of dry functionalized and non-functionalized hydrogel MNs. (B) Swelling ratio of functionalized and non-functionalized HMNs after immersion in ultrapure water for various time durations.

2.4.10. Capture BSA with the functionalized hydrogel

To assess the potential of MNs for capturing and detecting protein biomarkers, BSA was initially chosen as the target biomarker. Subsequently, HMNs were functionalized with anti-BSA antibodies and subjected to immersion in solutions containing BSA at varying concentrations. Following the capture of BSA using MNs, sABs were then introduced. The findings (Figure 2-7) from the BSA detection indicate that there is no significant variation in fluorescence intensity among the concentrations of 0, 10, and 20 $\mu\text{g/ml}$. A slight enhancement in fluorescence intensity was observed for the concentrations of 30 and 40 $\mu\text{g/ml}$. While this outcome shows promise, it necessitates further investigation and experimentation to ensure the precision of the detection process.

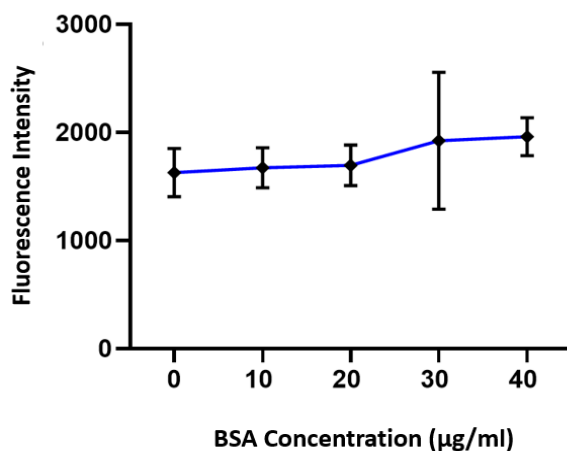


Figure 2-7. Capture and detection of BSA: The fluorescence intensity correlates with the amount of BSA capturing after immersion in BSA solutions with different concentrations.

2.5. Conclusion

This work introduces a novel HMNs that has been modified with antibodies. The central purpose of this MNs is to extract ISF from the skin and subsequently identify the biomarkers contained within the collected fluid. To perform this goal, HMNs were prepared and functionalized with antibodies using two various chemistry reaction, copper free click chemistry and EDC/NHS. The result of fluorescent intensity confirmed the bonding of antibodies to the hydrogel. To reinforce its validation, a labeled secondary antibody was employed. These promising findings underscored the HMNs potential for capturing and detecting protein biomarkers. However, the results of capturing could not definitively confirm the accuracy of this goal. Therefore, more investigations and complementary experiments are imperative to validate the detection mechanism.

2.6. References

1. Lee, H.J., A.W. Wark, and R.M.J.A. Corn, *Microarray methods for protein biomarker detection*. 2008. **133**(8): p. 975-983.
2. Caffarel-Salvador, E., et al., *Hydrogel-forming microneedle arrays allow detection of drugs and glucose in vivo: potential for use in diagnosis and therapeutic drug monitoring*. 2015. **10**(12): p. e0145644.
3. Miller, P.R., et al., *Extraction and biomolecular analysis of dermal interstitial fluid collected with hollow MNs*. 2018. **1**(1): p. 173.
4. Laszlo, E., et al., *Superswelling microneedle arrays for dermal interstitial fluid (prote) omics*. *Advanced Functional Materials*, 2021. **31**(46): p. 2106061.
5. Gong, H., et al., *Simple method to prepare oligonucleotide-conjugated antibodies and its application in multiplex protein detection in single cells*. 2016. **27**(1): p. 217-225.
6. Barker, K., et al., *Biodegradable DNA-enabled poly (ethylene glycol) hydrogels prepared by copper-free click chemistry*. 2016. **27**(1): p. 22-39.
7. Eeftens, J.M., et al., *Copper-free click chemistry for attachment of biomolecules in magnetic tweezers*. 2015. **8**: p. 1-7.
8. Goncin, U., et al., *Rapid copper-free click conjugation to lipid-shelled microbubbles for ultrasound molecular imaging of murine bowel inflammation*. 2022. **33**(5): p. 848-857.
9. Leung, M.K., et al., *Bio-click chemistry: Enzymatic functionalization of PEGylated capsules for targeting applications*. 2012. **124**(29): p. 7244-7248.
10. Jang, S., et al., *Development of a simple method for protein conjugation by copper-free click reaction and its application to antibody-free Western blot analysis*. 2012. **23**(11): p. 2256-2261.
11. Babity, S., et al., *A Naked Eye-Invisible Ratiometric Fluorescent Microneedle Tattoo for Real-Time Monitoring of Inflammatory Skin Conditions*. 2022. **11**(6): p. 2102070.
12. Bamgbelu, A., J. Wang, and J.J.T.J.o.P.C.A. Leszczynski, *TDDFT study of the optical properties of Cy5 and its derivatives*. 2010. **114**(10): p. 3551-3555.
13. Jing, P., T. Kaneta, and T.J.E. Imasaka, *Determination of dye/protein ratios in a labeling reaction between a cyanine dye and bovine serum albumin by micellar electrokinetic*

- chromatography using a diode laser-induced fluorescence detection*. 2002. **23**(15): p. 2465-2470.
14. Thakar, H., et al., *Biomolecule-Conjugated Macroporous Hydrogels for Biomedical Applications*. ACS Biomater Sci Eng, 2019. **5**(12): p. 6320-6341.
 15. Huynh, N.-T., et al., *Preparation and swelling properties of “click” hydrogel from polyaspartamide derivatives using tri-arm PEG and PEG-co-poly (amino urethane) azides as crosslinking agents*. 2013. **54**(4): p. 1341-1349.
 16. Myat, Y.Y., et al., *Fabrication and evaluation of thermally crosslinked Gantrez S-97 microneedle arrays*. 2020. **859**: p. 39-44.
 17. Dhiman, M., et al., *Formulation, characterization, and in vitro evaluation of bioadhesive gels containing 5-fluorouracil*. 2008. **13**(1): p. 15-25.
 18. Suriyaamporn, P., et al., *Computer-aided rational design for optimally Gantrez® S-97 and hyaluronic acid-based dissolving MNs as a potential ocular delivery system*. 2021. **61**: p. 102319.
 19. Kausar, A.J.J.o.P.F. and Sheeting, *Poly (acrylic acid) nanocomposites: Design of advanced materials*. 2021. **37**(4): p. 409-428.
 20. Kaczmarek, H. and M.J.T.O.P.C.J. Metzler, *The properties of poly (acrylic acid) modified with N-phenylbenzothioamide as potential drug carriers*. 2014. **6**(1).
 21. Tonghuan, L., et al., *Adsorptive features of polyacrylic acid hydrogel for UO 2 2+*. 2013. **297**: p. 119-125.
 22. Marini, I., et al., *Chaperone-like features of bovine serum albumin: a comparison with α -crystallin*. 2005. **62**: p. 3092-3099.
 23. Bjerneld, E.J., et al., *Pre-labeling of diverse protein samples with a fixed amount of Cy5 for sodium dodecyl sulfate–polyacrylamide gel electrophoresis analysis*. 2015. **484**: p. 51-57.
 24. Wang, L., et al., *Novel asymmetric Cy5 dyes: Synthesis, photostabilities and high sensitivity in protein fluorescence labeling*. 2010. **210**(2-3): p. 168-172.
 25. Yüce, M. and H. Kurt, *How to make nanobiosensors: surface modification and characterisation of nanomaterials for biosensing applications*. RSC advances, 2017. **7**(78): p. 49386-49403.

26. Hua, J., et al., *Preparation and properties of EDC/NHS mediated crosslinking poly (gamma-glutamic acid)/epsilon-polylysine hydrogels*. 2016. **61**: p. 879-892.
27. Nimse, S.B., et al., *Biomarker detection technologies and future directions*. *Analyst*, 2016. **141**(3): p. 740-755.
28. Donnelly, R.F., et al., *Hydrogel-forming MNs prepared from “super swelling” polymers combined with lyophilised wafers for transdermal drug delivery*. 2014. **9**(10): p. e111547.
29. Chandran, R., et al., *Factors influencing the swelling behaviour of polymethyl vinyl ether-co-maleic acid hydrogels crosslinked by polyethylene glycol*. 2022. **68**: p. 103080.
30. Waghule, T., et al., *MNs: A smart approach and increasing potential for transdermal drug delivery system*. 2019. **109**: p. 1249-1258.
31. Davis, S.P., et al., *Insertion of MNs into skin: measurement and prediction of insertion force and needle fracture force*. 2004. **37**(8): p. 1155-1163.
32. Peng, J., et al., *Polyamide nanofiltration membrane with high separation performance prepared by EDC/NHS mediated interfacial polymerization*. 2013. **427**: p. 92-100.

Chapter 2 -Supporting Information

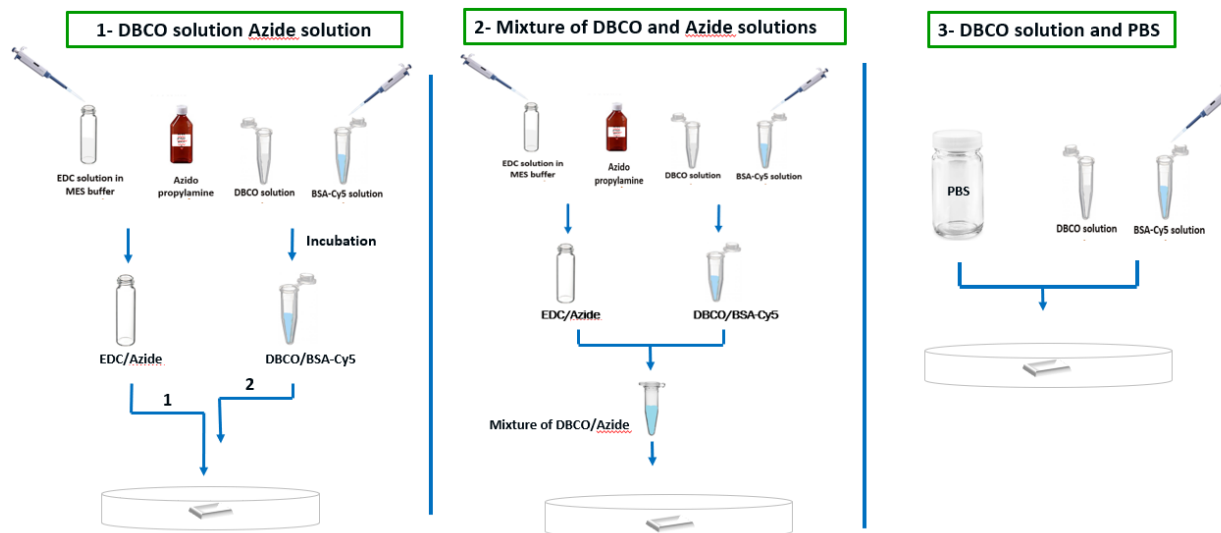


Figure 2-S1. Two various conditions for hydrogel functionalization with BSA; From left to right shows the addition of linkers to the hydrogel for the functionalization of hydrogel with BSA (first condition). 2- Preparing the mixture of linkers and adding it to the hydrogel for the functionalization with BSA. 3- Control samples.

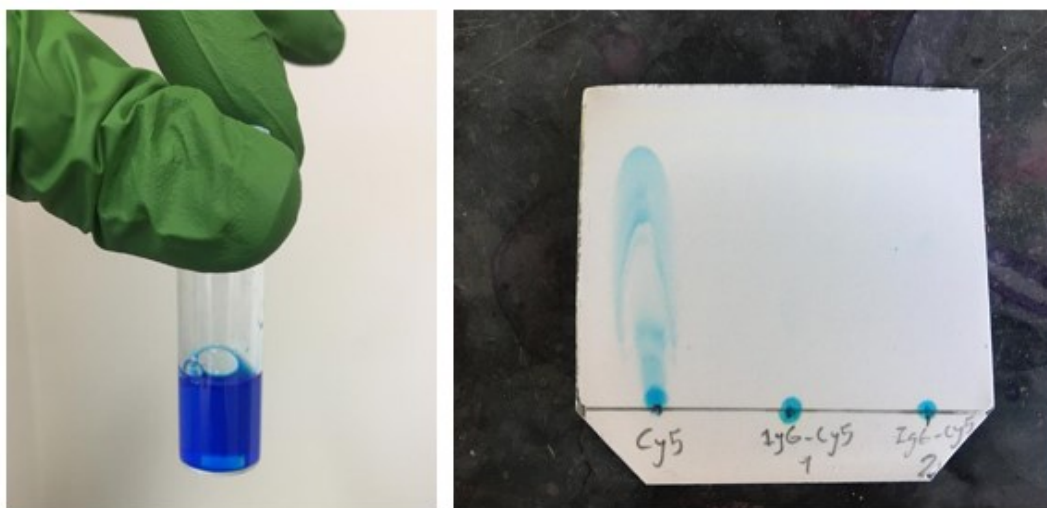


Figure 2-S2. TLC result: it is after purification.

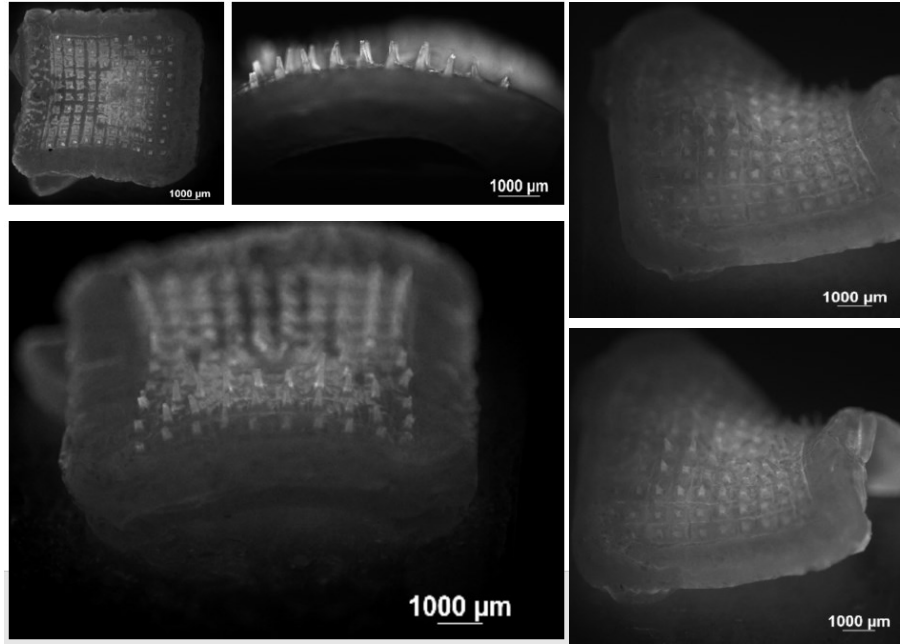


Figure2-S3. Hydrogel morphology after functionalization. Overall shape of the hydrogel samples (prepared by the first formulation) after functionalization with IgG-Cy5 using EDC/NHS.

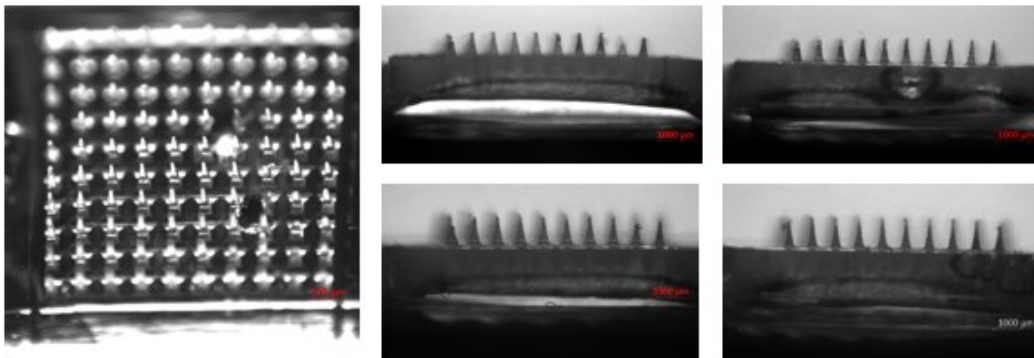


Figure 2-S4. MNs after mechanical test: Shape of the hydrogel MNs after mechanical compression force.

Chapter 3

3.1. Conclusion and outlook

The diagnostic field holds an irreplaceable position in healthcare, facilitating the prompt and precise identification of diverse medical conditions. Among a wide range of advance technologies, diagnostics provide critical insights into disease detection, progression, and treatment efficacy. Early diagnosis of disease leading to improved patient outcomes, reduced healthcare costs, and better resource allocation. Furthermore, diagnostics serve as a cornerstone for personalized medicine, tailoring treatments to individual patient profiles. With ongoing advancements in diagnostic tools, the field continues to revolutionize healthcare delivery by enhancing disease management, public health monitoring, and medical research endeavors. In the field of diagnosis, the identification of biomarkers plays a crucial role. The principal aim behind the biomarker detection is developing reliable and cost-effective tools for early diagnostic of disease that assist physician to choose more precise and accurate therapy. Moreover, it might help them within successfully tracking disease progression and recurrence. In this regard, there are various methods of biomarker's detection; most of them are immunoassay based methods [19]. Combination of immunoassay-based techniques into some medical tools make them appropriate for the biomarker detection [20, 21].

The employment of microneedle platforms for interfacing with ISF has gained significant attention as a promising approach for extracting tissue fluid from the dermis. MNs offers a minimally invasive route for the transdermal delivery of medicines that are typically too large to be absorbed through skin. HMNs is a category of MNs which provide unique advantages compared to other MN technologies. Their versatile design, self-disabling capability, and minimal risk of blockage offer clear benefits over alternative MN approaches used for monitoring purposes. Apart from their biocompatibility and biodegradability, these MN are able to remain intact and are removed without leaving any residue, even though they soften due to the absorption of ISF convenient [4, 12, 30, 32].

There are many important applications associated with MNs including drug delivery, ISF extraction and diagnostic field. Based on the literature, by incorporation or immobilization of

biomolecules (aptamers, antibodies, ...) into the MNs, it is possible to advance their application for diagnosis purposes such as detection of biomarkers from the skin [2].

Herein, antibody functionalized HMNs were developed with the aim of detecting protein biomarkers from the ISF. The synthesis and functionalization of HMNs were carried out utilizing two distinct chemical reactions, namely copper-free click chemistry and EDC/NHS. Notably, samples functionalized with a high concentration (1M) of EDC/NHS exhibited a more pronounced fluorescent intensity compared to alternative approaches, indicating the efficacy of this specific chemical method in achieving substantial functionalization. To reinforce the validation of these outcomes, a labeled secondary antibody was employed. These promising results underscore the potential of HMNs in capturing and detecting protein biomarkers. Indeed, the integration of hydrogel properties with biomolecules renders microneedles a promising tool for extracting interstitial fluid (ISF) and detecting specific protein biomarkers. This holds significant promise for the future, particularly in the realm of diagnosis. It could eliminate the use of hypodermic needles, prevent pain, injury, and irritation associated with their application [32]. In addition, the use of hydrogel-forming MN could practically eradicate the risk of infection, as the distended needles would be unable to pierce the skin of another patient upon intact removal, thereby eliminating the risk of needle-stick injuries [32]. For a more comprehensive exploration of the work, it would be valuable to functionalize the hydrogel with a pair of antibodies and identify their respective biomarkers. Additionally, by replicating the interstitial fluid (ISF) of the skin, it would be nice to verify specific protein biomarker among various biomarkers. This outcome would provide significant insights for subsequent *in vivo* experiments. Nonetheless, further investigations are imperative to substantiate the accuracy of these microneedles for *in vivo* detection, considering the intricacies of the body's environment, which may be influenced by various factors.

In conclusion, the future of MNs in the field of diagnosis holds immense potential for transformative advancements. MNs are poised to reshape diagnostics by offering innovative and patient-friendly sampling methods. These minimally invasive devices can efficiently extract biofluids, including ISF and blood, enabling the collection of valuable biomarkers. With the integration of cutting-edge sensing technologies, MNs can enable rapid and accurate on-site analysis, revolutionizing point-of-care testing. Their versatility extends to various applications, from continuous monitoring of chronic conditions to detecting infectious diseases and monitoring treatment responses. As research and development progress, MNs are expected to become more

refined, reliable, and accessible, making them a cornerstone of personalized and remote diagnostics.

3.2. References

1. Nimse, S.B., et al., *Biomarker detection technologies and future directions*. Analyst, 2016. **141**(3): p. 740-755.
2. Cao, Z., Y. Jia, and B. Zhu, *BNP and NT-proBNP as diagnostic biomarkers for cardiac dysfunction in both clinical and forensic medicine*. International journal of molecular sciences, 2019. **20**(8): p. 1820.
3. Hall, C., *NT-ProBNP: the mechanism behind the marker*. Journal of cardiac failure, 2005. **11**(5): p. S81-S83.
4. Caffarel-Salvador, E., et al., *Hydrogel-forming microneedle arrays allow detection of drugs and glucose in vivo: potential for use in diagnosis and therapeutic drug monitoring*. 2015. **10**(12): p. e0145644.
5. Turner, J.G., et al., *Hydrogel-Forming Microneedles: Current Advancements and Future Trends*. Macromolecular Bioscience, 2021. **21**(2): p. 2000307.
6. Madden, J., et al., *Biosensing in dermal interstitial fluid using microneedle based electrochemical devices*. Sensing and Bio-Sensing Research, 2020. **29**: p. 100348.
7. Zhang, X., et al., *Encoded microneedle arrays for detection of skin interstitial fluid biomarkers*. Advanced Materials, 2019. **31**(37): p. 1902825.
8. Yi, K., et al., *Aptamer-decorated porous microneedles arrays for extraction and detection of skin interstitial fluid biomarkers*. 2021. **190**: p. 113404.